Quantitative assessment of angiogenesis, perfused blood vessels and endothelial tip cells in the postnatal mouse brain

Wälchli, Thomas ; Mateos, José María ; Weinman, Oliver ; Babic, Daniela ; Regli, Luca ; Hoerstrup, Simon P ; Gerhardt, Holger ; Schwab, Martin E ; Vogel, Johannes

Abstract: During development and in various diseases of the CNS, new blood vessel formation starts with endothelial tip cell selection and vascular sprout migration, followed by the establishment of functional, perfused blood vessels. Here we describe a method that allows the assessment of these distinct angiogenic steps together with antibody-based protein detection in the postnatal mouse brain. Intravascular and perivascular markers such as Evans blue (EB), isolectin B4 (IB4) or laminin (LN) are used alongside simultaneous immunofluorescence on the same sections. By using confocal laser-scanning microscopy and stereological methods for analysis, detailed quantification of the 3D postnatal brain vasculature for perfused and nonperfused vessels (e.g., vascular volume fraction, vessel length and number, number of branch points and perfusion status of the newly formed vessels) and characterization of sprouting activity (e.g., endothelial tip cell density, filopodia number) can be obtained. The entire protocol, from mouse perfusion to vessel analysis, takes 10 d.

DOI: https://doi.org/10.1038/nprot.2015.002

Online summary: This protocol uses intravascular Evans blue labeling and Isolectin-B4 endothelial tip cell staining combined with antibody-based protein detection to monitor new blood vessel formation from tip cell selection to functional, perfused blood vessels.

Quantitative assessment of angiogenesis, perfused blood vessels and endothelial tip cells in the postnatal mouse brain

Thomas Wälchli[1,2,3], José Maria Mateos[4], Oliver Weinman[3], Daniela Babic[5], Luca Regli[2], Simon P. Hoerstrup[6], Holger Gerhardt[7,8,9], Martin E. Schwab[3], Johannes Vogel[10]

[1]Group of CNS Angiogenesis and Neurovascular Link, and Physician-Scientist Program, Swiss Center for Regenerative Medicine, University of Zurich, and Divisions of Neurosurgery and Surgical Research, University Hospital of Zurich, Moussonstrasse 13, CH-8091 Zurich, Switzerland; [2]Division of Neurosurgery and Laboratory of Molecular Neurooncology, University Hospital Zurich, Frauenklinikstrasse 10, CH-8091 Zurich, Switzerland; [3]Brain Research Institute, University of Zurich, and Department of Health Sciences and Technology, Swiss Federal Institute of Technology (ETH) Zurich, Winterthurerstrasse 190, CH-8057 Zurich, Switzerland; [4]Center for Microscopy and Image Analysis, University of Zurich, Winterthurerstrasse 190, CH-8057 Zurich, Switzerland; [5]Division of Cardiology, University Hospital Zurich, Raemistrsse 100, CH-8091 Zurich, Switzerland; [6]Swiss Center for Regenerative Medicine, University of Zurich, and Department of Surgical Research, University Hospital of Zurich, Moussonstrasse 13, CH-8091 Zurich, Switzerland; [7]KU Leuven, Department of Oncology, Vesalius Research Center, Vascular Patterning Lab, Herestraat 49, 3000 Leuven, Belgium; [8]VIB, Vesalius Research Center, Vascular Patterning Lab, Herestraat 49, 3000 Leuven, Belgium; [9]Vascular Biology Laboratory, London Research

Institute, Cancer Research UK, 44 Lincoln's Inn Fields, London WC2A 3LY, UK; [10]Institute of Veterinary Physiology, Vetsuisse Faculty, University of Zurich, Winterthurerstrasse 260, CH-8057 Zurich, Switzerland

Corresponding author:

Thomas Wälchli

Brain Research Institute

ETH and University of Zurich
Winterthurerstrasse 190
CH-8057 Zürich, Switzerland
Phone : +41 44 635 32 16
Fax : +41 44 635 33 03
E-mail: waelchli@hifo.uzh.ch

Group of CNS Angiogenesis and Neurovascular link

Swiss Center for Regenerative Medicine and Division of Neurosurgery

University and University Hospital Zurich
Frauenklinikstrasse 10
CH-8091 Zurich

thomas.waelchli@usz.ch

ABSTRACT

During development and in various diseases of the central nervous system (CNS), new blood vessel formation starts with endothelial tip cell selection and vascular sprout migration, followed by the establishment of functional, perfused blood vessels. Here, we describe a method that allows assessment of these distinct angiogenic steps together with antibody-based protein detection in the postnatal mouse brain. Intra- and perivascular markers such as Evans blue, Isolectin B4 or Laminin are used alongside simultaneous immunofluorescence on the same sections. Using confocal laser scanning microscopy and stereological methods for analysis, detailed quantification of the three-dimensional postnatal brain vasculature for perfused and non-perfused vessels (e.g. vascular volume fraction, vessel length and number, number of branch points, perfusion status of the newly formed vessels) and characterization of sprouting activity (e.g. endothelial tip cell density, filopodia number) can be obtained. The entire protocol, from mouse perfusion to vessel analysis, takes approximately 10d.

INTRODUCTION

The formation of new blood vessels can occur via different mechanisms[1-3]. Vasculogenesis describes the *de novo* formation of blood vessels during embryonic development, via differentiation of angioblasts (endothelial progenitor cells) into endothelial cells and subsequent assembly of these endothelial cells into a vascular network[1,2]. In contrast, sprouting angiogenesis is defined as the formation of new blood vessels from pre-existing ones, occurs throughout the entire life in various physiological and pathological conditions[1,2], and involves a range of complex cellular events such as cell adhesion, sprout initiation, migration, proliferation, tube formation and anastomosis[1,2]. A third – although less frequent - mechanism of physiological vessel formation that can also occur throughout the entire lifespan is the process of intussusception, during which pre-existing vessels split and give rise to daughter vessels[1,4,5]. The relative importance of these three modes of vessel formation varies between organs[1,2,6].

Angiogenesis in the postnatal mouse brain

In the mouse CNS, vascularization starts with formation of the perineural vascular plexus via vasculogenesis at the ventral neural tube at around embryonic day 7.5 – 8.5 (E7.5 – E8.5)[7-9]. Subsequently, at around E9.5, endothelial sprouts emerging from the perineural vascular plexus invade the CNS parenchyma in a caudal to cranial direction and vascularize the CNS tissue mainly via sprouting angiogenesis[7-10]. While these vessel sprouts migrate towards the ventricles, further sprouting and branching of the newly formed vessels takes place, thereby forming the CNS vessel network[7,9]. This occurs not only during embryonic development of the CNS[7,9] but also continues at the postnatal stage[11,12]. Postnatally, sprouting angiogenesis and vascular branching further expand and remodel the three-dimensional CNS vasculature[11,12]. Other perivascular cell types such as vascular smooth muscle cells and

pericytes are recruited and finally stabilize the newly formed blood vessels[5,10] thereby establishing the mature functional CNS vasculature[4,7].

The vascular network of the CNS parenchyma is established via sprouting angiogenesis which is driven by a subset of endothelial cells found at the leading edge of the vascular sprout that are called endothelial tip cells. These cells sense with their filopodia environmental cues to guide the blood vessel sprout towards gradients of angiogenic growth factors like VEGF or bFGF[1,2]. Tip cells are followed by endothelial stalk cells, which proliferate and form the vascular lumen, thereby elongating the vascular sprout[1,2,13,14]. After fusion of neighboring sprouts, lumen formation allows perfusion of the newly formed vessel[1,2,15-18]. Subsequently, endothelial cells in the newly formed blood vessels resume a quiescent state, the so-called phalanx cells, and the now mature blood vessel reaches a functional stage[1,2,19]. Importantly, vessels that are unable to become perfused, regress[1,2,20].

Towards mature, perfused blood vessels – the postnatal mouse brain as a model

During postnatal brain development, angiogenesis is quite active[11,12,21,22], thus, providing an interesting model system to study sprouting angiogenesis, the predominant mode of vessel formation in the brain[7,8]. Similar to axonal growth cones, endothelial tip cells are guided by the interplay of attractive and repulsive cues involving for instance the axonal guidance molecules Netrins, Semaphorins, Slits and Ephrins as well as the neural growth inhibitor Nogo-A[3,8,12]. An increased number of vascular sprouts and endothelial tip cells can result in an increased number of perfused blood vessels[23] as we have for instance shown for animals lacking functional Nogo-A[12]. Initially, the balance between endothelial tip and stalk cell numbers and the balance between tip migration and stalk proliferation affect branching frequency and plexus density[24]. The transition from sprouting endothelial tip cells to functional, perfused blood vessels is mainly regulated by the VEGF-VEGFR-Dll4-Jagged1-

Notch pathway[1,2,13,18,24-26]. Disturbance of these processes can lead to non-productive angiogenesis and aberrant blood vessels[23,26-29]. However, the final functionally perfused vascular network seems to be remodeled depending on many factors including metabolic and mechanical feedback from the surrounding tissue and the flowing blood respectively[20], that are not completely understood so far[18]. For example, in tumor angiogenesis, blockade of Dll4-Notch signaling that normally limits the number of tip cells and filopodia leads to more filopodial protrusions and finally more blood vessels. However, these vessels are hypo- or non-perfused, e.g. not functional, thus resulting in reduced instead of the initially expected increased tumor growth[26,28-30]. Consequently, vessel density and tumor growth showed no correlation in these studies[26,28-30].

These findings underline the need for a detailed analysis to address the different angiogenic steps including endothelial tip cell selection, vascular density and perfusion status of blood vessels. Presently there is no established protocol to precisely and quantitatively distinguish between perfused and newly forming blood vessels including vascular endothelial tip cells. However, such a protocol is crucial in order to investigate the mechanical and metabolic feedback finally responsible for maturation as well as for stability of functional vascular networks[20]. Precise co-localization of the perfusion status of the (newly forming) capillaries with endothelial tip cell morphology as well as with the molecular machinery driving angiogenesis has been problematic, contributing to the incomplete current knowledge on vascular network maturation. The protocol presented here addresses this issue and correlates the *in vivo* perfusion status of the vasculature (not postmortem perfusion of fixed animals) with angiogenic events in the three-dimensional (3D) vascular network of the developing postnatal mouse brain.

Development of the protocol

Capillary development in the postnatal rat brain has been described previously[11] and the analysis of total versus perfused vascular network in the adult rat brain was analyzed using a combination of immunfluorescence staining against Fibronectin (FN) to visualize the total vessel tree and intravascular Evans blue (EB) injection to label perfused vessels[31]. Recently, we have identified Nogo-A as a negative regulator of angiogenesis and endothelial tip cell number in various regions of the postnatal mouse brain by using IB4 to label the existing vessels as well as endothelial tip cells and intravitally injected EB to assess the portion of perfused vessels[12]. However, in this study, EB^+ and $IB4^+$ vessel structures were quantified using a computer-controlled, microscope stage on 10 µm coronal brain sections, whereas the number of endothelial tip cells was addressed in a separate group of mice on 40 µm free-floating coronal brain sections using a different staining- and fixation protocol optimized to visualize endothelial tip cells and their filopodial protrusions[12].

Here, we demonstrate an optimized combination of these methods, thereby allowing simultaneous visualization and quantification of endothelial tip cells, the total vascular network and functional, perfused blood vessels. Using design-based stereological methods we provide absolute parameters characterizing the postnatal 3D mouse brain vessel network.

Applications of the protocol

The presented protocol distinguishes between $EB^+/IB4^+$ perfused vessels and the total $IB4^+$ vasculature including newly formed vessel sprouts with endothelial tip cells (vascular sprouts are $EB^+/IB4^+$ or $EB^-/IB4^+$). Importantly, the method can be combined with immunofluorescence to correlate the expression of virtually any protein of interest with the developing 3D vessel structures. The protocol can be used to study the influence of any angiogenic or other molecule in relation to the ratio of perfused and non-perfused vessels and endothelial tip cells in the postnatal mouse brain. Moreover, pro- or anti-angiogenic effects of pharmacological compounds, peptides or blocking antibodies on the developing postnatal

brain vasculature can easily be tested in wild-type or genetically modified mice[12] and quantitatively characterized using computer-aided stereological methods (e.g. provided by IMARIS, ImageJ, Steroinvestigator, CAST, Stereologer or comparable software). Finally, given that angiogenesis plays a crucial role not only during tissue development but also in various pathologies in- and outside the CNS[1,2,8,42,43] such as hypoxia or malignancies[8], the method presented here could - after validation in other tissues or pathological conditions - be applied in these settings.

Overview of the procedure

Here, we present a technique for the visualization and quantification of vascular endothelial tip cells and functionally perfused vessels in the postnatal mouse brain, Figure 1 shows the flow chart of the procedure along with a timescale. The protocol starts with preparation of the solutions needed and continues with intracardial Evans Blue injection at the desired day of postnatal development (in our case P8), followed by brain dissection, immersion-fixation, cryoprotection, cryostat cutting, immunofluorescent stainings, imaging and quantification of vascular structures using stereology.

The step-by-step procedure of intracardial EB injection and brain dissection is illustrated in Figure 2a-h and in Supplementary Videos 1 and 2). As a first step, mice (e.g. P8) are intracardially injected with 6 µl/g body weight of 2% Evans blue. A 30.5G needle is used and positioned above the heart ca. 2 mm parasternal to the left at a virtual line connecting both armpits, in a caudal and lateral angle of 30° and 10°, respectively (Fig. 2a-b and Supplementary Video 1). Successful injection is followed by immediate bluish appearance of the paws, snout and tail (Fig. 2c and Supplementary Video 1). After 5–10 min., the brains are dissected out of the skull (Fig. 2d-f and Supplementary Video 2) and cut into three coronal pieces of ~2 mm thickness (Fig. 2g,h) that are then immersion fixed in 4% formaldehyde (FA)

solution made from paraformaldehyde (PFA) with varying contents of glutaraldehyde (GA) (two possibilities: 0.025% GA, or 0.05% GA) overnight. This fixation step and especially the addition of GA retains the Evans blue in the vessels (see Supplementary Fig. S1 and Tissue fixation) and preserves the tissue to allow immunofluorescent staining (see Supplementary Fig. S1). After cryoprotection in 30% (w/v) sucrose in 0.1M PB for 2-3 days, brain sections are cut and processed free-floating for IB4, DAPI and immunofluorescence staining. We have obtained best results with the antigens selected here (e.g. to address blood vessels and perivascular cells, see Supplementary Fig. S3) when the primary antibodies were incubated (together with IB4 and DAPI) for three days, followed by incubation with secondary antibodies overnight (Supplementary Fig. S3, Table 2). Finally, the sections are mounted, imaged with a confocal laser scanning microscope and quantitatively analyzed using stereological methods.

We recommend the use of relatively thick (e.g. 40 μm) brain sections to obtain reliable 3D information about the blood vessel tree and to quantify vessel parameters such as vessel volume fraction, vessel length or vessel branch points (Fig. 5). In addition, more endothelial tip cells appear complete (including its entire filopodial tree) in these 40 μm thick brain sections (Figs. 3, Fig. 4, Fig. 5, Fig. 6), thereby allowing a complete 3D reconstruction of filopodia and quantitative analysis including filopodia number, length and straightness (Fig. 6).

Experimental design

This protocol describes the visualization and quantification of vascular endothelial tip cells and functionally perfused vessels in the postnatal mouse brain. Figure 1 shows the flow chart of the procedure along with a timescale. The protocol starts with preparation of the solutions needed and continues with intracardial Evans Blue injection at the desired day of postnatal development (in our case P8), followed by brain dissection, immersion-fixation,

cryoprotection, cryostat cutting, immunofluorescent stainings, imaging and quantification of vascular structures using stereology.

The step-by-step procedure of intracardial EB injection and brain dissection is illustrated in Figure 2a-h and in Supplementary Videos 1 and 2). First, mice (e.g. P8) are intracardially injected with 6 µl/g body weight of 2% Evans blue using s 30.5G needle that is positioned above the heart ca. 2 mm parasternal to the left on a virtual line connecting both armpits, in a caudal and lateral angle of 30° and 10°, respectively (Fig. 2a-b and Supplementary Video 1). Successful injection results in immediate bluish discoloring of paws, snout and tail (Fig. 2c and Supplementary Video 1). After 5–10 min., the brains are dissected out of the skull (Fig. 2d-f and Supplementary Video 2), cut into three coronal pieces of ~2 mm thickness (Fig. 2g,h) and immersion fixed overnight in 4% formaldehyde (FA) solution made up of paraformaldehyde (PFA) with varying contents of glutaraldehyde (GA) (two possibilities: 0.025% GA, or 0.05% GA). This fixation step and especially the addition of GA retains the Evans blue in the vessels (see Supplementary Fig. S1 and Tissue fixation) and preserves the tissue to allow immunofluorescent staining (see Supplementary Fig. S1). After cryoprotection in 30% (w/v) sucrose in 0.1M PB for 2-3 days, brains are sectioned and processed free-floating for IB4, DAPI and immunofluorescence staining. We have obtained best results with the antigens selected here (see Table2, Supplementary Fig. S3) when the primary antibodies were incubated (together with IB4 and DAPI) for three days, followed by incubation with secondary antibodies overnight. Finally, the sections are mounted, imaged with a confocal laser scanning microscope and quantitatively analyzed using stereological methods.

We recommend using relatively thick (e.g. 40 µm) brain sections to obtain reliable 3D information about the blood vessel tree as a prerequisite to quantify vessel parameters such as vessel volume fraction, vessel length or branch points (Fig. 5). In addition, more complete endothelial tip cells can be found in thicker brain sections (Figs. 3, Fig. 4, Fig. 5, Fig. 6),

thereby allowing 3D reconstruction of their entire filopodia tree and its quantitative analysis including filopodia number, length and straightness (Fig. 6).

Experimental animals. This protocol can be applied to mice of various postnatal ages; we have used P8 here. However, it should be kept in mind that genetic or other manipulations (e.g. intraperitoneal antibody or tamoxifen injections) can affect the growth (and in consequence the weight) of animals[44]. Therefore, it is important to measure the animal weight prior to EB perfusion because similar weights (and ages) ensure best a comparable developmental stage (especially for mouse pups). Because the postnatal development of the vasculature is quite fast[11], the developmental stage of the mice need to be carefully controlled. To this end, age and weight of the animals has to be precisely measured. Littermate controls should be used where available but weight match of the animals seems to be an even more important parameter with regard to vessel structure analysis since many genetic modifications can as a side effect alter the overall postnatal development[45].

In accordance with previous reports[9], we recommend to use at least 6 animals per groups. In general, the more pronounced a difference between two test groups is, the smaller the number of animals to detect this effect becomes and vice versa. When analyzing postnatal CNS angiogenesis and vasculature in genetically modified mice, it is essential to incorporate the appropriate controls, e.g. including brains from postnatal wild-type littermates. All animal procedures must be carried out in accordance with the guidelines outlined by the institutional and cantonal review committees for animal experiments.

Evans blue injections. Evans blue binds non-covalently and in low concentrations almost completely to serum albumin[46]. Thus EB stays in place after fixation of all proteins in the sample including the intravascular albumin. Therefore, we intracardially inject mice with a rather low amount of 6 µl/g body weight of 2% Evans blue that sufficiently stains the

vasculature because it is bound almost completely to albumin. At the same time the injected amount is low enough to prevent EB diffusion into the brain tissue[31,46]. The brains are then dissected out of the skull and cut into three coronal pieces (Figure 2g,h) to facilitate immersion-fixation in 4% FA + 0.025% GA or in 4% FA + 0.05% GA overnight. This fixation had to be optimized in order to fulfill two requirements: i) to retain the Evans blue in the vessels and, ii) to preserve the tissue by fixation but not "over-fixing" the tissue to allow simultaneous visualization of endothelial tip cells and a variety of antigens by immunofluorescence (Supplementary Figure S1).

Tissue cutting. For tissue cutting, the brain slices are cut into 40 µm coronal sections on a cryostat for free-floating processing. For navigation within the postnatal mouse brain tissue, we refer to the Developing Mouse Allen Brain Atlas (http://developingmouse.brain-map.org/docs/Overview.pdf) (alternatively, any other Brain Atlas can be used) or used alternating sections stained with cresyl violet (Nissl stain).

Tissue fixation. We have optimized the simultaneous visualization of perfused blood vessels (visualized with Evans blue) and of the total vessel tree including forming blood vessels and vascular endothelial tip cells with their filopodia (stained with biotinylated Isolectin B4 (IB4)) using different methods of immersion fixation after Evans blue perfusion.

Previously, after having acquired the EB pictures (for the visualization of the perfused blood vessels) in the adult rat brain, EB was washed out by rehydratation[31], followed by subsequent FN staining to visualize the total (perfused and non-perfused) vessel structures. Moreover, for the combined analysis of EB^+ perfused blood vessels and $IB4^+$ total vessels (including forming vessel sprouts), a specific in-house-developed computer-controlled microscope stage was needed that allowed the relocalization of the regions of interest after FN staining and EB washout[31]. In addition, FN antibodies did not label endothelial tip cell (filopodia)[31].

Moreover, the visualization of endothelial tip cells and the filopodial tree in the postnatal mouse brain that we have developed to address the comparison of these structures between P8 WT and P8 Nogo-A KO animals[12] was initially performed on brains from animals that were intracardially perfused with 4% FA[12], a procedure that would wash away the Evans blue.

In improving the two above-mentioned methods, we were faced with two problems:

- how to retain the EB in the tissue if a fixation step using FA in aqueous solution was necessary (for good tissue fixation including the endothelial tip cells). An aqueous FA solution would wash away the intravascular EB[31].
- how to maintain tissue preservation and to visualize endothelial tip cells in the fragile postnatal mouse brain tissue if an intracardial perfusion with 4% FA was not possible, because it would wash away the intravascular EB.

In order to allow the simultaneous visualization of EB^+ perfused blood vessels and $IB4^+$ total vessels including endothelial tip cells, we tested the following combinations of formaldehyde (FA) and Glutaraldehyde (GA) fixatives (Supplementary Fig. S1a-d): i) 4% FA + 0.25% GA, ii) 4% FA + 0.05% GA, iii) 4% FA + 0.025% GA and iv) 4% FA alone (no GA). When using 4% FA alone (no GA) for immersion-fixation, EB was less well retained in the tissue (Supplementary Fig. S1a-d). In contrast, the use of 4% FA + 0.25% GA decreased the detection sensitivity of endothelial tip cells and especially of their filopodial protrusions. The best results for EB-IB4 double visualizations were obtained using 4% FA + 0.05% GA and 4% FA + 0.025% GA. These combinations also worked well for several antibody stainings, e.g. for pericytes (PDGFRβ), astrocytes (GFAP), neurons (Nf160), microglia (Iba1) and the basement membrane (Laminin) (see Fig. 3g-j, Supplementary Fig. S3 and Table 2 antibodies). After cryoprotection in sucrose for 2-3 days, brain sections are cut on a cryostat, taken up in buffer and processed free-floating for immunofluorescence staining.

Antigen retrieval, background reduction and permeabilization. To decrease background staining, a blocking step using either normal serum from the species in which the secondary antibodies were raised or IgG-free and protease-free BSA is performed. It is important to check the compatibility of the blocking serum with the secondary antibody used. For instance, when using primary goat antibodies, one has to replace the normal goat serum of the blocking reagent with 2-4% normal horse serum or with IgG-free BSA at 0.5-2%. Permeabilization steps are important to improve the antibody/marker penetration into the tissue. We permeabilize sections in 0.3% Triton-X for 10 min and use primary antibody solution containing 0.05 % Triton-X. We have experienced better endothelial tip cell filopodia stainings by introducing the following antigen retrieval steps: Briefly, brain sections are incubated in 50 mM NH_4Cl in 0.1M phosphate buffer for 30 min at 22°C, followed by incubation in 50 mM glycine in 0.1 M Tris (pH 8.0) for 5 min at 80 °C in a microwave (600W) to quench aldehyde groups. For antigen unmasking, sections are then incubated in $CaCl_2$-containing buffer (0.1 mM $CaCl_2$ + 0.1 mM MgCl2 + 0.1 mM MnCl diluted in 0.1M PBS (pH 6.8)) and heated three times for 30s in a microwave (600 W). Furthermore, the specificity of the different antibody stainings has to be validated using species-specific IgG control antibodies or secondary antibody alone stainings. In addition, verify the absence of the signal in a knockout model (if available) or otherwise mimic the knockout phenotype using specific inhibitors and blocking peptides.

Vascular labeling. We have obtained best results when antibody staining and biotinylated IB4 were incubated for three days, followed by incubation with secondary antibodies overnight and sufficient washing steps. The brain vasculature is labeled with biotinlyated IB4 (as a marker of the total vascular network), with Laminin (as a marker for blood vessels with a basement membrane) as well as with *in vivo* intracardially injected Evans blue to visualize perfused vessels[46]. IB4 from the african-based black bean *Griffonia simplicifolia* binds with

high affinity to α-galactosyl residues of glycoproteins on the cell surface of the endothelium[47-51], thereby allowing the visualization of blood vessel endothelial cells including endothelial phalanx, stalk and tip cells as well as endothelial tip cell filopodia in various tissues[9,49,52,53]. For the visualization of endothelial tip cell filopodia, we obtain the best results when using biotinylated IB4 diluted 1:50 (20 µg/ml) in $CaCl_2$-containing buffer combined with streptavidin–Cy3/streptavidin-Alexa Fluor 543/streptavidin-Dye-light 547 diluted 1:200 in $CaCl_2$-containing buffer (see paragraph "procedure") (Figs. 3-6). Notably, in addition to endothelial cells, (biotinylated) IB4 also labels macrophages/microglial cells (Fig. 3g-j), as previously described[54,55] and we also observed $IB4^+$ microglial cells with the staining protocol described here (Fig. 3g-j). To distinguish microglial cells and tissue macrophages from endothelial cells, macrophages/microglial cells can specifically be labeled with an anti- Iba1-antibody (Fig. 3g-j). Laminin is a protein to visualize the basement membrane of blood vessels walls[1,31] and can be recognized by an anti-Laminin antibody (see Table 2). Evans blue is a dye that non-covalently binds to serum albumin and thereby allows investigation of functional, perfused vessels[31,56]. Perivascular cell types of the neurovascular unit such as pericytes, astrocytes, neurons and microglia can be stained by corresponding cell type-specific antibodies (see Fig. 3, Supplementary Fig. S3 and Table 2 antibodies).

Imaging and quantification. To optimally address the 3D postnatal brain vasculature, we use confocal laser scanning microscopy. EB^+ and $IB4^+$ vessel structures, volume fraction, length and the number of branch points and endothelial tip cells can be quantified with lower magnifications (20x, NA 0.7). The resulting images are analyzed using the Stereoinvestigator Software (Fig. 5).-Visualization and analysis of endothelial tip cell filopodia is performed by acquiring 3D stacks using high numerical aperture objectives (e.g. 63x, NA 1.4, Figure 3c-f, Figure 4, Figure 6). To analyze endothelial tip cell filopodia (see Box 1), we use the image processing software Imaris 7.6.2 (Bitplane) (Fig. 6, Box 1). Briefly, filopodia are traced by

the filament module (Figs. 4,6, Box 1) obtaining the following parameters: filopodia number per tip cell, filopodia length and filopodia straightness (Fig. 6).

Design-based stereological methods provide direct information about morphological 3D parameters of interest, e.g. the length of vessels, the number of vessel branch points or the vessel volume fraction. This is in stark contrast to the biologically difficult to interpret but commonly used variety of measures like "percent of the area of a section occupied by vessels", "number of pixels occupied in an image" or "measures of length or diameter" in 2D projections. The term "Design-based" refers to the mathematical bases of these methods. They are mathematically ("proofable", not empirically) designed to return an accurate value of the parameter of interest. If one is interested in vessel length, e.g, spaceballs will return the accurate vessel length in the material at hand independent of the orientation, diameter or tortuosity of the vessels. They are, like all other methods, only limited by the ability of an observer to recognize the structures that are to be measured[32].

Design-based methods are typically presented as "package deals", i.e. a combination of a particular sampling approach (where to measure) with specific probes (how to measure). "Uniform random systematic sampling" is the generally best choice of sampling because of its efficiency. Using this approach, the tissue is probed at regular (systematic) intervals. In the case of tissue sections, these intervals are typically predefined distances along the x- and y-axes of the sections. To make the sample statistically representative, the first location at which the tissue is investigated must be located at random within the first sampling interval. Thereafter this tissue is investigated at the systematic intervals that were defined. If n measures the need to be performed to obtain a desired precision with a random independent sample, typically √n measures, and, therefore, a √time necessary to perform the measurements, will be sufficient using a uniform random systematic sample[33,34].

The easiest mode of how to measure is to count the interactions between vascular features and geometric probes, i.e. how many times does a test point fall onto the volume of a vessel, how many times does the length of a vessel intersect with a test area or how many vessel branch points are contained in a volume probe. Very simple relationship equations[33,35] are used to convert these counts of interactions to volume, length and number densities, which can then be converted to absolute values if the reference volume (ROI volume) or the sampling fraction is known. If , e.g., capillaries perforate the surface of 50 spaceball probes[36] with a surface of 10000 μm^2 each 70 times (Q = 70), the relationship equation L_V (length density) = $2Q/A$ = 140/(50×10000 μm^2) provides a length density estimate of 0.00028/μm^2. If the ROI has a volume of 1 mm^3 (10^9 μm^3), an estimate of the total length of capillaries in the ROI is 0.00028/μm^2 × 10^9 μm^3 = 280000 µm. Specialized software packages such as for example Stereoinvestigator that we have used here have the advantage that all calculations are taken care of. Both, introductory reviews[35,37-39] and comprehensive and comprehensible basic texts[33,40] that explain design-based stereological methods and that include extensive example calculations are available.

Aside from their rigorous mathematical basis and efficiency, design-based stereological methods provide access to parameters that would otherwise be difficult if not impossible to accurately measure in tissue sections. For instance, we estimated the length of capillary segments to have a length of 325 µm. Direct measurements would require the inclusion of the entire capillary segment in the section plane. In 40 µm thick tissue sections, capillaries that course perpendicular to the section plane cannot be measured, potentially biasing estimates to capillary segments with a preferred orientation (in the section plane). Tortuous capillary segments would be more likely to be interrupted by the section plane than straight ones, potentially biasing estimates to capillaries of a certain shape. Shorter capillary segments would be more likely included in the section than longer ones, always generating an

underestimate independent of orientation and shape. Any experimental intervention that alters the orientation or shape of capillary segments, i.e. 3D vascular architecture, has the potential to change estimates of segment length in an unpredictable direction and with unpredictable strength and, most importantly, without the need for an actual change of length to be present. Aside from obviating the need to generate a sufficiently large sample of capillary segments included in the section plane in the first place, the combination of stereological length estimates[40] with branch point counts[41] to derive segment length is free from these potential biases.

Advantages of the protocol compared to alternatives

The analysis of functional, perfused blood vessels, newly forming blood vessels and endothelial tip cells in the postnatal mouse brain described here has several key advantages as compared to other methods:

- This method enables to quantitatively distinguish, simultaneously and within the same specimen, between newly forming blood vessels including endothelial tip cells and mature, perfused vessels[11,12] (Figs. 4,5,6).
- The protocol used here allows simultaneous immunofluorescence in combination with the analysis of the perfusion status of the vasculature and the detection and analysis of vascular endothelial tip cells (Fig. 3g-j, Figs. 4,5 and Supplementary Fig. 2). In contrast, previous protocols dealing with the distinction between EB^+ perfused and $IB4^+$ or FN^+ total blood vessels[11,12], a subsequent analysis of the EB^+ and $IB4^+$ or FN^+ total vessel structures required serial sections or sequential processing of the sections and a precise re-localization of the analyzed vessel tree between different sections or imaging

procedures[11,12] Furthermore, a simultaneous analysis of endothelial tip cells on the same slides was not possible due to the different fixation protocols.,

- Methods to analyze angiogenesis and endothelial tip cells in- and outside the CNS have been described for the embryonic mouse hindbrain[9], the postnatal mouse retina[44,57], and the embryonic zebrafish intersegmental vessels (ISVs)[58,59]. Moreover, perfused vessels and tip cells have been addressed in the retina[23,53] and a recent study investigated vessel perfusion in the postnatal mouse brain[22] but did not show a simultaneous visualization and quantification of the sprouting activity. Given the relevance of postnatal brain angiogenesis[11,12], the concomitant lack of adequate methods to study these processes and the still limited knowledge of regulators of postnatal brain angiogenesis[12,21], our method enlarges the armamentarium to study sprouting angiogenesis from the postnatal retina to the postnatal mouse brain.
- Stereological analysis of confocal z-stacks allows the accurate analysis of the 3D vessel structure in the postnatal mouse brain, i.e. it produces true vessel parameters (e.g. at P8; see Fig. 5) with direct biological meaning such as true vessel length in a defined volume of tissue instead of difficult-to-interpret measures like “percentage of section area occupied by vessels”. In contrast, the often-used analysis of maximum intensity projections of tissue slides can for example lead. to an overestimation of the vessel density, an error that increases with section thickness. Thus, in principle, 3D analysis and stereological methods[41] resulting in true vessel volume fractions provide more accurate quantifications and allow better comparison of different studies.
- In contrast to section analysis (2D, maximum intensity projections), analysis of 3D images obtained from confocal z-stacks using stereological methods allows retrieval of additional characteristics of the vascular network such as vessel volume fraction, vessel length and number, number of branch points, number of filopodia, filopodia length and straightness and number thereof per endothelial tip cell (Fig. 5j-n).

- Our protocol allows clear identification of endothelial tip cells, based on morphological criteria (see Figs. 3,4,5,6). Several markers for endothelial tip cells such as VEGFR2, VEGFR3, Dll4, CxCR4 and CD34 have been proposed in recent years[1,2,8,60-66]. However, there is currently no marker available that selectively labels endothelial tip cells, as all the above-mentioned markers also label stalk cells, even though to a lesser extent (Suppplementary Fig. S2a-l). IB4 also labels tip and stalk cells, the rest of the vascular endothelium as well as microglial cells but using our protocol, the filopodial tree of tip cells is nicely displayed thereby allowing tip cell identification. In contrast, the suggested tip cell markers VEGFR2, VEGFR3 and Dll4 did not label the entire filopodia tree (Supplementary Fig. S2) and would not allow a detailed analysis of the filopodia morphology (Fig. 6a-t). Accordingly, the best method to detect endothelial tip cells is still based on morphological criteria, e.g. a vascular sprout extending numerous filopodia forming "hand-like" structures (e.g. about 8-25 filopodia per cell, Figs. 4,5,6).The combination of IB4 with a microglia-specific marker such as Iba1 allows to clearly distinguishing microglial cells from endothelial tip cells (Fig. 3g-j, Fig. 4d-f). In addition, endothelial tip cells are most often found at the end of non-perfused - thus EB^- - capillaries (Fig. 4d-f, Fig. 6).
- High resolution confocal microscopy enables to visualize, quantify and characterize endothelial tip cell filopodia and to obtain quantitative parameters such as number of filopodia per tip cell, filopodial length and filopodial straightness (Fig. 6q-t).
- The present protocol can be combined with immunofluorescence using various other vascular markers, e.g. pericyte markers (PDGFRβ, CD13), astrocyte markers (GFAP) or neuronal markers (Nf160 and TubβIII) to visualize perivascular cell types (see Supplementary Fig. S3), whereas basement membrane markers (Laminin, Fibronectin) allow to address yet another feature of vascular maturation, namely the establishment of a vascular basement membrane (Fig. 4,5 and Suppplementary Fig S3). In principle, virtually

any protein of interest can be analyzed in the morphological context of the developing vascular network (see Table 2 for antibodies that we have tested). This was not possible with earlier methods[11,12]. Finally, the technique described here is relatively easy and fast to perform and provides highly reproducible results.

Limitations of the method described here

Despite the advantages described above, the method also has some disadvantages and limitations:

- In contrast to the superficial vascular plexus of the postnatal retina[44,57] that forms a two-dimensional flat vascular structure that can easily be assessed, imaged and analyzed, in principle even with a standard fluorescence microscope, the postnatal mouse brain vasculature develops in 3D with vessel sprouting occurring in all directions. Consequently, for proper analysis, confocal imaging is mandatory resulting in much longer image acquisition times and larger data sets. The structural complexity of the postnatal mouse brain requires precise navigation within each individual sample in order to assure that equivalent brain areas are selected, cut, analyzed and compared. This is important because the vascular density and most likely also timing and angiogenic activity varies considerably between the brain regions[11]. Navigation within postnatal mouse brain samples as prepared with the present protocol is hampered because no standard histological stain such as Nissl or H&E (which would disturb the immunofluorescence) can be applied on the same sections. Therefore, for detailed navigation, we recommend to refer to the Developing Mouse Allen Brain Atlas or to other commonly used Brain Atlas (see also Fig. 3a).

- Although the method enables to distinguish between endothelial tip cells, newly formed but yet immature blood vessels and functional, perfused vessels, blood flow passing through the functional vessels cannot be measured. This is of relevance because it has been shown that an increased density of perfused blood vessels does not necessarily result in a higher blood flow, e.g. as shown for transgenic overexpression of $VEGF_{165}$ (= VEGF-A) in the adult mouse brain[67,68].
- This protocol provides only snapshots of brain angiogenesis at different time-points for individual mice and therefore requires a large number of animals to study dynamics of angiogenesis over time. However, methods to study *in vivo* angiogenesis in the developing postnatal mouse brain are currently not widely available. In principle, nevertheless, methods for "real-time" imaging of the brain vasculature exist[69-71] and may in future complement our protocol.
- Similar to the methods addressing angiogenesis in the embryonic hindbrain and postnatal retina, the distinction between tip cells and trailing stalk cells is not always clear with our method. For example, at the retinal front, it can be difficult to identify which filopodia belong to which tip cell. In the postnatal brain, even though endothelial tip cells appear very clearly (Fig. 3,4,5,6), it is difficult to precisely delineate the borders between different cells.
- Although diffusion of the intravascularly injected EB into the brain tissue is limited by binding of the EB dye to the much larger plasma proteins and the short circulation time, some dye extravasation cannot be excluded, for example in experimentally induced pathological conditions associated with an impaired blood brain barrier (e.g. stroke, brain trauma or malignancies/brain tumors). However, during postnatal mouse brain development, we never observed significant EB extravasation around vessel structures including angiogenic active vessels that that are supposed to be more leaky more leaky than mature vessels, e.g. at the tip cell or directly adjacent vascular segments (cf. Figs. 4i,

5b,c,g-i, 6b,g,k,o).Further improvements of the method could include markers of lumen formation and endothelial polarization[13,18,72,73], as well as new, highly selective markers for endothelial tip and stalk cells.

MATERIALS

REAGENTS

- Isoflurane 5% in oxygen (IsoFluo, Abott, code B506)
- 10 ml Syringe (Braun)
- Evans blue dye (Sigma-Aldrich, cat. no. E2129, Dye content ≥ 75%)
- Paraformaldehyde (PFA; Sigma-Aldrich. cat. no. P6148)
    - ! CAUTION This and some of the chemical substances mentioned below are harmful if inhaled and swallowed and are irritating to the eyes, respiratory system and skin. They may cause sensitization of skin upon contact. Therefore, in principle, wear protective goggles, clothing and gloves as appropriate. Use the chemicals in a fume hood. Carefully read the safety sheets of all chemicals used in this protocol.
- Glutaraldehyde (GA 25%; Polyscience cat.no.01909)
    - ! CAUTION It is harmful if inhaled and swallowed. GA is irritating to the eyes, to the respiratory system and to the skin. It may cause sensitization of skin upon contact. Wear protective goggles, clothing and gloves as appropriate. Use it in a fume hood.
- Saline solution
    - 0.9% NaCl in distilled water
- 0.1M Phosphate Buffered Saline (0.1 M PBS)
    - or PBS tablets (Sigma-Aldrich, cat. no. P4417
- Triton X-100 (Sigma-Aldrich, cat. no. T8787)
    - ! CAUTION It is harmful if ingested and can cause serious damage to the eyes. Wear protective goggles, clothing and gloves as appropriate.
- 0.1M Tris(hydroxymethyl)aminomethane buffer (Tris; VWR, cat. no. 443864E)
- Biotinylated Isolectin from Bandeiraea simplicifolia BS-I Isolectin B4 (IB4; final concentration: 20 µg·mL−1; Sigma-Aldrich, cat. no. L2140)
    - CRITICAL The protocol has been optimized for this lectin (e.g. to visualize endothelial cells and endothelial tip cell filopodia), and its use is therefore recommended. Biotinylated IB4 provided a higher signal-to-noise ratio as compared to non-biotinylated IB4. This was especially important to detect endothelial tip cell filopodia.
- DAPI (1:40,000, Sigma-Aldrich, cat. no. D9542)

- Primary antibodies

    - CRITICAL The protocol has been optimized for the primary antibodies listed below (e.g. to visualize astrocytes, (GFAP) pericytes (PDGFRβ), the basement membrane of blood vessels (Laminin), neurons (Nf160) and microglia/macrophages (Iba1)) and it is therefore recommend to use these antibodies.

- Rabbit anti-GFAP antibody (1:1,000; DAKO Cytomation, cat. no. Z0334)

- Rat anti-PDGFRβ antibody (1:200; eBioscience, cat. no. 12 1402)

- Rabbit anti-Laminin antibody (1:250; Sigma-Aldrich, cat. no. L9393)

- Rat anti-mouse Nf160 antibody (1:250; Zymed, cat. no. 13-0700)

- Rabbit anti-mouse/human Iba1 antibody (1:250, Wako, cat. no. 019-19741)

- Rabbit anti-VEGFR2 antibody (1:1,000; Cell Signaling, cat. no. 2479)

- Goat anti-VEGFR3 antibody (1:1,000; R&D Systems, cat. no. AF743)

- Rabbit anti-Dll4 antibody (1:1,000; R&D Systems, cat. no. MAB1389)

- Secondary antibodies

    - CRITICAL The protocol has been optimized for the secondary antibodies listed below and it is therefore recommend to use these antibodies. However, it is possible to choose alternative (streptavidin-conjugated) fluorophores.

- DyLight 594-conjugated streptavidin (1:200, Jackson Laboratories, cat. no. 016-500-084?

- Horseradish peroxidase (HRP)-tagged rabbit anti-rat secondary antibody (Dako, cat. no. P045)

- HRP-tagged streptavidin (Dako, cat. no. P0397)

- Alexa Fluor 488–conjugated goat anti-rabbit secondary antibody (1–2 μg·mL−1, Life Technologies, cat. no. A11034)

- Alexa Fluor 488–conjugated goat anti-mouse secondary antibody (1–2 μg·mL−1, Life Technologies, cat. no. A11032)

- Alexa Fluor 488–conjugated goat anti-rat secondary antibody (Life Technologies, cat. no. A11006)
- Alexa Fluor 488–conjugated donkey anti-goat secondary antibody (Life Technologies, cat. no. A11055)
- 8-day-old mouse pups (WT/Bl6, male or female).
    - CAUTION: Institutional and governmental ethics regulations concerning rodent use must be followed
- Mounting medium (Dako, cat.no.53023)
- 2-Methylbutane (Sigma-Aldrich M32631)
- Tissue Tek (Sakura, cat.no. 4583)
- Nail Polish (colorless, Migros Switzerland)
- Distilled water (aqua milipore, MilliQ Synthesis A10) MILLIPORE
- 5M NaOH
- Filter paper (Schleicher & Schuell, Type LS14 1/2)
- Reagent A NaH2PO4 * H20 (Axon lab, Appli Chem, Cas-No 10049-21-5, Ec-nNo.: 2314492)
- Reagent B Na2HPO4 * 2H20 (Axon lab, Appli Chem, Cas-No.: 10028-24-7, Ec-nNo.: 2314487)
- Bl6C57 mice, postnatal day 8 (P8)

EQUIPMENT

- Falcon tubes, 15 ml (BD Falcon, cat. no. 35-2099)
- Falcon tubes, 50 ml (BD Falcon, cat. no. 352074)
- 24 well plates (Millipore, cat. no. PSHT010R1)
- Glass superfrost slides (Menzel Gmbh, cat.no. J1800AMNZ)
- Dissecting instruments: scissor (Fine Science Tools, cat. no. 14079-10), forceps (Fine Science Tools, cat. no. 11065-07), dissection forceps no. 5 (Fine Science Tools, cat. no. 91150-20), spring scissors (Fine Science Tools, cat. no. 15000-10)
- Dissection microscope (Zeiss OPMI1, Zeiss)

- Fluorescence microscope (Leica MZ16 F, Leica) coupled to a digital camera (Hamamatsu C4742-95, Hamamatsu)
- Confocal laser scanning microscope SP5 (Leica SP5, Leica)
    - CRITICAL The protocol has been optimized with this confocal microscope, but it is possible to choose alternative confocal microscopes (e.g. from Olympus or Zeiss) C
- Imaging editing software: IMARIS 7.6.4 software (Bitplane Scientific software), Adobe Photoshop CS3 or CS5 (Adobe)
- Stereology software: StereoInvestigator 11.0 software (mbf Bioscience)
- Transfer pipettes (Sarstedt, cat. no. 86.1171)
- Erlenmeyer flasks, 250 ml
- Tabletop balance (e.g. ED Presicion balance, Sartorius)
- Cryostat (e.g. indications)
- Water bath (e.g. Stuart SWB15D, Stuart)
- Tilting table

REAGENT SETUP

- **Evans blue solution (2%, wt/vol)**: Add 200mg of Evans blue to 10ml of 0.9% saline. and vortex for 3-5min. The solution should be aliquoted and can be stored at -20°C for unlimited time. Thaw an aliquot at room temperature (20-25°C) for use. If an aliquot is not used up completely it can be re-frozen.
- **Formaldehyde solution (FA) (4%, wt/vol in 0.1M PB)**: Under a chemical fume hood, weigh 8 g of paraformaldehyde (PFA)powder into an Erlenmeyer flask and add 100 ml distilled water (aqua milipore). Dissolve the PFA powder by heating the solution (containing a clean magnetic stir bar) to 60 °C to facilitate dissolving the PFA powder, add few drops of 5 or 10M NaOH when mixing starts. After PFA powder dissolved completely, filter the FA solution using a filter paper. To dilute the 8% FA solution to the final concentration of 4% FA in 0.1M PB, add 100 ml of 0.2M PB. When the solution has cooled down to room temperature, check the pH and adjust to pH 7.4 if necessary. Aliquots can be stored at − 20 °C for ~3 weeks[44] up to 1 year[9], however, we recommend to freshly prepare the 4% FA solution for every experiment. Thaw the aliquots at room temperature or at 37 °C in a water bath and cool them to 4° C on ice before use.
- **Glutaraldehyde solution (GA) (0.05% or 0.025%, wt/vol)**: Dilute from GA stock 25% into the 4% FA solution. The GA stock solution can be stored at room temperature for years.

- **PB (PBS) solution (0.2M)**: Under a fume hood, weigh 5.24g of reagent A and 18.83g of reagent B into a 1l bottle and add 1000 ml of distilled water (aqua milipore). Dissolve this 0.2M PB solution by stirring using a magnetic stir bar until reagents A and B have completely dissolved. Check the pH and adjust to pH 7.4 if necessary. To obtain 0.1M PBS, dissolve 8g NaCl and add 500 ml of distilled water to 500ml of the 0.2M PB solution. PB or PBS should be stored at room temperature for not more than three months.
- **Fixation solution (4% FA + 0.025% or 4% FA + 0.05% GA)** : Add GA from the 25% GA stock soluation into the 4% FA solution to yield final concentrations of 0.025% GA or of 0.05% GA in 4% FA, respectively.
- **50 mM NH4Cl in 0.1M PB**: Dissolve 0.26g ammonium chloride (Merck 1145) in 50 ml distilled water added to 50 ml 0.2M PB. Storage at room temperature for less than three months.
- **50 mM glycine in 0.1 M Tris (pH 8.0)**: Dissolve 0.38g glycine (Sigma,G8898) and 0.3g TRISMA Base (Sigma T6066-5 Kg) in 100ml dest. water and adjust pH to 8.0. Storage at room temperature for less than three months.
- **CaCl-containing staining buffer:** Add 0.1mM $CaCl_2$, 0.1 mM $MgCl_2$ and 0.1 mM MnCl to 0.1M PBS (pH 6.8) (slightly modified from Gerhard et al., *J Cell Biol*, 2013[53]). Microwave heating solution and primary and secondary antibody solution. Storage at room temperature for less than three months.
- **Permeabilization solution**: Add 0.3% Triton X-100 to 0.1 M Tris-buffered saline solution (pH 8.0) and stir overnight at room temperature. Storage at room temperature for less than three months.

EQUIPMENT SETUP

- **Tilting table:** The tilting table should be placed in a fridge or in a cold room, as antibody incubations for primary antibodies and for biotinylated IB4 should be performed at 4 °C. Incubation with secondary antibodies can alternatively be performed at room temperature.
- **Confocal microscopes:** Laser scanning confocal microscopes equipped with -at least - 4 laser lines (405 nm; 488 nm; 568 nm and 633 nm) and spectral detectors to separate the different fluorochromes were used. For the experiments described here, we used a SP5 confocal microscope (Leica Microssystems) but similar instruments from other companies can be used. Image stacks were acquired with 20x NA… or 63x NA 1.4 objectives using an image format of 1024 x1024 pixels. Voxel size for the high-resolution images was: 80 x 80 x 170 nm. We used sequential scan to detect the nuclei stained with DAPI using a 405 nm laser, for IB4 a 561 nm laser and for Evans blue a 633 nm laser. The detectors (HyD detectors (Leica) at 12 bit) were set between 417- 476 nm, 568 - 674 nm, and 641- 747 nm respectively. For colocalisation studies of blood

vessel endothelial cells and perivascular cells and -structures, e.g. astrocytes (e.g. using GFAP as marker), pericytes (e.g. using PDGFRβ as marker), neurons (e.g. using Nf160 as marker), microglia/macrophages (e.g. using Iba1 as a marker) or the basement membrane (e.g. using laminin as marker), combinations of primary antibodies and secondary antibodies labeled with Alexa 488 can be used.

- **Stereoinvestigator**: see steps 32-37 in "Procedure"
- **Imaris**: see steps 38-39 in "Procedure"

PROCEDURE

Animal perfusion with Evans blue (day 1) TIMING ~5-10 min per animal

1. Anaesthetize P8 mice using 5% Isoflurane in 100% oxygen for 3-5 min. To this end put the animal into a syringe (usually they crawl by themselves into the syringe) connected to the Isoflurane vapor).
    - CAUTION**:** Animal procedures must be carried out in accordance with relevant institutional and governmental ethics guidelines.
2. When the animal is properly anesthetized (test with tail punch) pull it back out of the syringe so that only its head stays inside the syringe and turn it on its back. Under a dissecting stereomicroscope, puncture the heart of the animal with a 30.5 G needle about 3mm cranial to the xiphoid process and 2mm parasternal (to the left) in an angle of about 30° caudally and 10° to the left of the animal, about 5mm deep and inject 6µl per g body weight of 2% (wt/vol) Evans blue dissolved in saline (Fig. 2a,b and Supplementary Video 1).
    - CRITICAL STEP: the Evans blue injection is successful if the animal gets immediately bluish. This can be particularly well monitored at the paws, snout or tail of the animal (Fig. 2c and Supplementary Video 1)
    - CRITICAL STEP: Push the needle fast into the animal. Do not worry that you push it too deep because in this case it is no problem to retract the needle slightly. Use each needle only once as they should be sharp. If you fail to hit the heart the first time retract the needle completely and try once more.

Dissection of the brain (day 1) TIMING ~5 min per animal

3. Decapitate the perfused animal with a scissor and dissect the brain out of the skull using a fine scissor and a forceps. Carefully incise the skull at its lateral sides, starting posterior (cerebellum) all the way to anterior (bulbus olfactorius), on both sides of the skull (Fig. 2d and Supplementary Video 2).
    - CRITICAL STEP: Perform the skull dissection carefully by keeping the scissor blade that is located inside the scull away from the brain surface (Fig. 2d and Supplementary Video 2). Otherwise, this may cause damage to the brain tissue.
4. Remove the skull from the brain tissue by pulling gently away using a forceps (Fig. 2e and Supplementary Video 2). Separate the brain from the inferior part of the skull by cutting the optic and other nerves using a forceps in order to facilitate brain tissue removal (Fig. 2f).

- CRITICAL STEP: Prevent tension on the brain tissue while removing the skull from the brain. Pay attention to also remove residual tissue of the dura mater (Fig. 2e and Supplementary Video 2).

5. Cut the isolated brain into three coronal pieces e.g., according to the lines shown in Fig. 2g using a sharp scalpel or razor blade (Fig. 2h), in order to facilitate fixation.
    - CRITICAL STEP: brain regions which will be dedicated for stereological analysis should be kept intact
6. If the experiment requires genotyping of the litter, keep a piece of the animal tail for genomic DNA isolation.

Immersion fixation of the brain tissue (day 1) TIMING ~over night

7. Transfer the isolated coronal brain pieces (Fig. 2h) immediately into 15ml of freshly prepared, cold 4% (wt/vol) FA + 0.025% (vol/vol) or 4% (wt/vol) FA + GA/0.05% (vol/vol) GA on ice. Place only one brain into 15 ml fixative.
    - CRITICAL STEP: Do not allow the brain tissue to dry out. Thus, transfer it to the fixative immediately. Use plenty of fixative (e.g. 15 ml per mouse brain as suggested here) in order to improve fixation.
    - CRITICAL STEP: For all antibodies mentioned in this protocol (Table 2 antibodies), freshly prepared or freshly thawed fixative containing 4% FA and 0.025% GA or 4% FA and 0.05% GA is a suitable fixative. Other antibodies may require alternative fixation protocols.
8. Fix the samples overnight at 4°C and proceed to the cryoprotection

Cryoprotection of the brain tissue (days 2-3) TIMING ~1-2 days

9. Remove fixative and add 15ml freshly prepared, cold 30% (wt/vol) sucrose in 0.1M PBS to the brain tissue (coronal brain sections). Place the brain sections in a fridge at 4°C and store them for 2-3 days.
10. After 2-3 days (when the brain samples have sunk to the bottom of the 15ml falcon tube), remove the excess of sucrose from the sample by gently touching the surface of the brain with a filter paper.
    - CRITICAL STEP: Do not allow the brain tissue to dry out. Thus, the transfer from the 30% sucrose to the Tissue Tek has to be quick.
11. Put the coronal brain piece to a small aluminum foil container plastic mold filled with Tissue Tek and label the rostral and the dorsal parts.

- CRITICAL STEP: The orientation of the brain tissue is crucial for finding later the desired brain structures. Pay attention to correctly align the brain tissue in a rostral to dorsal manner.

12. Put the coronal brain piece in Tissue Tek to 2-methylbutane at a temperature of -40°C. Remove the brain sample of the 2-methylbutane and immediately label the sample. Put all samples of them into a plastic bag labeled with the animals name, and put this plastic bag on dry ice
    - CRITICAL STEP the temperature of the N-methylbuthane should be precisely -40°C (max. +/- 2°C) as guarantees an optimal and homogeneous freezing of the samples without tissue cracking. .
    - CRITICAL STEP: these steps have to be quick as temperature changes can alter the quality of the brain tissue
13. If you plan sectioning the brain not instantly but within the next 1-3 days, store the tissue at -20°C. If longer storage is desired, keep the brain tissue at -80°C.
    - PAUSEPOINT: In our experience, storing the brain tissue at -80°C is superior to storing the brain tissue at -20°C. At -80°C, brain tissue can be stored without quality loss more than one year. However, put the brain tissue from -80°C to -20°C prior to cutting (otherwise, the brain tissue is to fragile/brittle for cutting; see below).

Cutting of the brain tissue (starting on day 3-5) TIMING ~1 hour per animal

14. If you stored the brain tissue at -80°C put it 2-4h prior to cutting brain sections to -20°C (either in the cryostat or a -20°C freezer)
    - CRITICAL STEP: If the tissue is too cold the sections will crumble while cutting.
15. Within the cryostat, remove the brain tissue from the aluminum foil container or plastic mold used for freezing and mount it in a rostral to dorsal orientation using Tissue Tek.
16. Adjust the temperature settings of the cryostat (tissue block: -20°C, knife/cryostat chamber: -20°C)
17. Cut the brain tissue into 40 µm thick coronal sections and transfer them with a brush into a well of the 24 well plate filled with 0.1M PB at room temperature (free floating sections), for orientation to the desired brain structures, we suggest the sources listed in Table 1.
    - CRITICAL STEP: 40 µm thick sections constitute an optimal sections thickness to assure both the 3D visualization of endothelial tip cell filopodia as well as an adequate antibody penetration. After being transferred to 0.1M PB, the sections should flatten out/deroll and not fall apart in the 0.1M PB

Table 1: Developing mouse Allen Brain Atlas (P4 and P7)

Developmental stage, stain and cutting plane	**Web-link**
P4, overview	http://atlas.brain-map.org/atlas#atlas=181276162&plate=100711203&structure=16382&x=4840&y=3720&zoom=-5&z=3
P4, NISSL, sagittal	http://developingmouse.brain-map.org/experiment/thumbnails/100033295?image_type=nissl
P4, NISSL, coronal	http://developingmouse.brain-map.org/experiment/thumbnails/100034998?image_type=nissl
P7, NISSL, sagittal	http://developingmouse.brain-map.org/experiment/thumbnails/100073790?image_type=nissl
P7, NISSL, coronal	http://developingmouse.brain-map.org/experiment/thumbnails/100098039?image_type=nissl

18. Collect the 40 µm coronal sections in a 24 well plate filled with 0.1M PB (0.5 ml -1 ml per well)

Staining procedure (starting on day 6) TIMING ~5 days

19. Remove the 0.1M PB from the 24 well plates using a pipette.
20. Postfix the P4 or P8 40-µm coronal free-floating sections for 10 min in either 4% (wt/vol) FA in 0.1M PB (P8 animals) or in 4% (wt/vol) FA, 0.05% GA in 0.1M PBS (P4 animals) (0.5 ml – 1 ml per well) depending on the desired antibody staining.
    - CRITICAL STEP: For maintaining the EB in place, GA added to the FA appears to be superior (Supplementary Fig. S3). Moreover, addition of 0.05% GA to the P4 coronal brain tissue sections ensures the stability of the brain tissue at this younger age
21. Start antigen retrieval by incubating the sections in 50 mM NH_4Cl in 0.1 M phosphate buffer for 30 min with gentle shaking (100 rpm) on an table (at room temperature).
22. Incubate the sections in 50 mM glycine in 0.1 M Tris (pH 8.0) for 5 min with gentle agitation on a tilting table at 80 °C
23. Perform microwave heating (600 W) in CaCl2-containing buffer [0.1mM CaCl2 0.1mM MgCl2 0.1mM MnCl diluted in 0.1MPBS (pH 6.8), slightly modified according to[53]] for 30s up to 1.5 min.
    - CRITICAL STEP: antigen retrieval (and unmasking using microwave heating in particular) assures in our hands a better detection of endothelial tip cell (filopodia)
24. Permeabilize the sections in 0.1 M Tris-buffered saline. 0.3% Triton X-100 for 10 min with gentle shaking on a table at room temperature.

25. Incubate the sections for 72h with gentle shaking on an inclined table at 4°C in primary antibodies diluted in CaCl2-containing buffer and blocking solution (0.05% Triton X-100 and 2% (vol/vol) normal goat serum (NGS) in 0.1M PBS) using primary antibodies or biotinylated IB4 (Table 2), respectively. The best alternative is excess normal serum from the species in which the secondary antibodies were raised.
26. Thoroughly wash the sections three times in 0.1M PB/0.1M PBS for 5-10 min each with gentle shaking on an inclined table at room temperature
27. Incubate the sections with gentle shaking on an inclined table overnight at 4°C in secondary antibodies diluted in CaCl2-containing buffer and blocking solution (0.05% Triton X-100 and 2% (vol/vol) normal goat serum (NGS) in 0.1M PBS)
28. Thoroughly wash the sections three times in 0.1M PB/PBS for 5-10 min each with gentle shaking on a tilting table at room temperature
29. Mount the sections onto labeled glass slides. Transfer the sections one by one to a dish with clean 0.1M PBS using a brush. Within this PBS-containing dish, carefully transfer the free floating coronal sections onto a clear glass slide
    - CRITICAL STEP: Perform this step with the glass slide submerged at half in a 0.1M PBS-containing dish to prevent surface tension from rupturing the sections. This is – due to the fragility of the tissue - particularly relevant for mounting sections of mice at ages of P4 and P8 (less crucial for coronal sections of adult mice)
30. Do not submerge the already mounted coronal sections into PBS, as they will detach again otherwise. Mount 3-5 (ideally: 4) coronal sections onto a clear glass slide using MOWIOL mounting medium. Add a coverslip on top of the sections, remove the residual liquid on the edges of the cover slip using a tissue (Kleenex) and seal the coverslip using Nail Polish. Store the slides in dark at 4°C.

Imaging (day 10-12) TIMING ~variable (entire confocal stacks, endothelial tip cells etc.)

31. Identify the region of interest (for more detailed information, see paragraph “Cutting of the brain tissue”)
32. Image the fluorescently labeled coronal brain sections using a confocal laser scanning microscope (e.g. in our case, we were using (SP5 and SP8, Leica Confocal Microscopes and a OLYMPUS Fluoview 1000 Confocal Microscope)
    - CRITICAL STEP: For low magnification images and reference images use low NA objectives as 10x. For the tip cells and filopodia we were using 63x NA1.4 or similar objectives.

Quantitative 3D analysis (day 10-12) TIMING ~variable (depending on the parameters to analyse - entire confocal stacks, endothelial tip cells etc.)

33. Quantitative 3D analysis consists of two parts:

Characterisation of the blood vessel network (stereological analysis,), see step 34, options A-E, and Figure 5) and Characterisation of endothelial tip cells and their filopodia (isosurface generation, , filament tracing,see step 35, options A,B, and Figure 6)

Characterisation of the blood vessel network - Stereological analysis TIMING 4h per mouse

34. Assess vascular features quantitatively by their interaction with geometrical probes, i.e. points for vascular volumes, areas for vascular lengths and volumes for vascular branch points[36,41]. Use design-based stereological methods because the resulting estimates are unbiased in the sense that the number of interactions is independent of the size, shape or orientation of vascular features other than that of the feature of interest[74].

- CRITICAL STEP: The Region of Interest (ROI) was defined to comprise a complete cortical transect from the pial surface to the deep border of layer VI of a 40µm thick coronal brain section of a P8 mouse that was perfused with Evans blue (EB) and stained with biotinylated Isolectin B4 (biotinylated IB4) (see Fig. 5a-f). StereoInvestigator 10 (MBF Bioscience, Williston, VT)was used to apply the probes to the confocal image stacks. Sampling was uniform random systematic.
- CRITICAL STEP: Sampling parameters depend on both the size of the ROI and the densities of vascular features. They can be adjusted following the principles outlined by[33,75-79]. We recommend choosing parameters, as we did it here to provide approximately 100 sampling sites within the area of the image stacks and an average of 1-3 probe/feature interactions per probe. For data presentation, extrapolate all estimates to a volume of one cubic millimeter (Fig. 5j-n).

Depending on the user's interest, follow option A for vessel volume fraction, option B for vessel length, option C for vessel branchpoints, option D for vascular endothelial tip cells and option E for derived vascular parameters/values.

(A) Vessel volume fraction

To estimate the volume fraction occupied by all vessels and by perfused vessels use the Area Fraction Fractionator[80,81] (Fig. 5d,g). Here estimates were performed on randomly selected single optical planes (0.2µm thick) from confocal z-stacks to minimize over-projection errors. We used one plane of each stack.

(i) Superimpose a 100 × 100 µm lattice of points spaced 8 µm apart to the ROI in this plane at sampling locations separated by 200 µm along the x- and y-axis (Fig. 5d,g).

(ii) If a point (of the above-mentioned lattice) fell onto an $IB4^+$ vessel structure (morphologically excluding $IB4^+/Iba1^+$ microglia structures (Fig. 5g, left side), next assess the Evan's blue (EB) channel (Fig. 5g, right side). If the vessel structure was $IB4^+/EB^+$ (IB4/EB double-positive), count the point as perfused vessel volume; if the vessel structure was only $IB4^+$, count the point as non-perfused vessel volume (Fig. 5g). Base all volume estimates on the appearance of the vessel in the IB4 channel. Count all other points of the lattice and within the ROI as reference volume.

(B) Vessel length

To estimate total and perfused vessel length, use spaceballs[36], i.e. isotropic surfaces in the form of hemispheres (Fig. 5e,h). We recommend the following substeps:

(i) Generate hemispheres with a radius of 20 µm within the ROI of the image stacks at sampling locations separated by 70 µm along the x- and y-axis (Fig, 5h).

(ii) Assess each crossing of an $IB4^+$ vessel and the circles representing the circumferences of a hemisphere (Fig. 5h, left side) in the Evan's blue channel (Fig. 5h, right side). Counting crossings as belonging to perfused or non-perfused vessel length according to the (ii) criteria in point 32. If a $IB4^+$ vessel structure or a EB^+ vessel structure was out of focus, the intersection was not counted (Fig. 5h, lower row).

(C) Vascular branch points

To estimate the number of vascular branch points for all and perfused vessels, use the Optical Fractionator[74] (Fig. 5f,i, upper row). To this end:

(i) Place optical dissector samples sized 100 × 100 × 20 µm within the ROI of the image stacks at sampling locations separated by 150 µm along the x- and y-axis (Fig. 5i, upper row).

(ii) Categorize branch points according to the number of vascular branches that originate from them and count separately. We only observed branch points comprising either 3 or 4 branches.

(iii) Assess each branch point of an $IB4^+$ vessel (Fig. 5i, upper row, left side) in the Evan's blue channel (Fig. 5i, upper row, right side). Count vascular branch points as belonging to perfused or non-perfused

vessel length according to the criteria (ii) . If a $IB4^+$ vessel structure or a EB^+ vessel structure is out of focus, do not count the intersection (Fig. 5h, lower row).

(D) Vascular endothelial tip cells

The Optical Fractionator[74] should also be used to estimate the number of vascular endothelial tip cells (Fig. 5i, lower row). To this end:

(i) Place optical dissector samples sized 100 × 100 × 20 µm within the ROI of the image stacks at sampling locations separated by 150 µm along the x- and y-axis. .(Fig. 5i, upper row)

(ii) Define $IB4^+$ endothelial tip cell cells as following: $IB4^+$ vessel structures with a clearly defined tip cell body, from which a filopodia tree containing numerous filopodia emerge (Fig. 5i, lower row, left side; see also Fig. 4 and Fig. 6). As endothelial tip cell filopodia are not visible in the Evan's blue channel (Fig. 5i, lower row, right side), endothelial tip cells cannot be addressed in the Evans blue channel. If an $IB4^+$ vessel structure is out of focus, the intersection should not be counted (Fig. 5h, lower row).

(E) Derived vascular parameters/values

i) If desired, calculatee derived vascular parameters/values such as average diffusion distances, average capillary segment number, average capillary segment length and average capillary segment radius. These calculations are implemented in the software used (Stereoinvestigator) according to the formulas provided in[41] (Fig. 5g, lower row).

Characterisation of endothelial tip cells and their filopodia - Isosurface generation and filament tracing TIMING 30 min per endothelial tip cell

35. Perform quantitative analysis of endothelial tip cell filopodia using Imaris software and the filament tracing module therein. Further qualitative morphological information is obtained by rendering the fluorescence signal of blood vessels to generate isosurfaces. The resulting isosurfaces allow to better distinguish the body of the vessel sprout from the endothelial tip cell filopodia.

Follow option A for isosurface generation and option B for filament tracing.

(A) Isosurface generation

To generate isosurfaces, use the "surface" function in Imaris.

(i) Identify the area of interest (e.g. cerebral cortex, hippocampus, etc.).

(ii) Identify endothelial tip cells in the sample using the microscope using a high NA objective (e.g. 63x, NA.1.4).

(iii) Acquire image stacks of endothelial tip cells using an image format of 1024 x1024 pixels. Voxel size: 80 x 80 x 170 nm. Use a sequential scan to detect the nuclei stained with DAPI using a 405 nm laser, for IB4 use a 561 nm laser and for Evans blue use a 633 nm laser. We set the detectors between 417- 476 nm, 568 - 674 nm, and 641- 747 nm respectively. We used HyD detector (Leica) at 12 bit.

(iv) Open the image stacks with Imaris and use the "surface" function to generate rendered volumes of the blood vessels. Select the "source channel" from which the surfaces are to be processed (e.g. the "EB channel" for perfused blood vessels or the "IB4 channel" for the entire vessel network). Check the "smooth" option to apply a Gaussian filter to the dataset and select a Surface area detail level. Large values will generate smoother and less detailed surfaces, the value should fit the detail level of the fluorescent structure.

(v) Perform a "background substraction" to estimate the background intensity value of each voxel. Isosurfaces are generated according to a certain "threshold intensity level". The "manual thresholding" allows a fitting of the isosurface to the fluorescent data.

(vi) Control the generated isosurfaces using filters. There are many filters, but "volume" and "intensity" are the most useful ones. The "volume filter" filters out too small or too large false volumes and the "intensity filter" can separate isosurfaces by their intensity values.

(vii) The rendered isosurface volumes facilitate the filopodia tracing as the starting point of endothelial tip cell filopodia can better be defined.

(B) Filament tracing (filopodia analysis)

The filopodia analysis includes the analysis of filopodia number, filopodia length and filopodia tortuosity/straightness. To analyse filopodia, use the "filament" function in Imaris.

(i) Identify the area of interest (e.g. cerebral cortex, hippocampus, etc.).

(ii) Identify endothelial tip cells in the sample using the microscope using a high NA objective (e.g. 63x, NA.1.4).

(iii) Acquire image stacks of endothelial tip cells using an image format of 1024 x1024 pixels. Voxel size: 80 x 80 x 170 nm. Use a sequential scan to detect the nuclei stained with DAPI using a 405 nm laser, for IB4 use a 561 nm laser and for Evans blue use a 633 nm laser. We set the detectors between 417- 476 nm, 568 - 674 nm, and 641- 747 nm respectively. We used HyD detector (Leica) at 12 bit.

(iv) Open the image stacks with Imaris (Bitplane) and use the “filament” function to trace the filopodia. We have used the autopath function to trace the filopodia. Alternatively, the software provides a manual and a more automatic function as well. We recommend the autopath function as a compromise between the fully automatic and the fully manual functions. In this mode, the origin of the filopodium is selected with a mouse click. Then, the filopodium can be traced by moving the mouse to the end of this filopodium, The software shows the trace of that particular filopodium in 3D. In this way, all visible filopodia emerging from one endothelial tip cell can be identified.

- CRITICAL STEP: Whereas a fully automatic function is prone to errors due to the overlapping filopodia, a fully manual function, on the other hand, is very time consuming. The autopath function is a compromise between these two options: the researcher identifies the origin of the filopodia and the software provides a preview tracing along the volume of fluorescence filament candidates. Then, the researcher confirms the pre-traced filopodia by examination in fully 3D mode. Using the autopath function, it can be assured that the filopodia tracing is correct and feasible within a realistic time frame.

(v) From Imaris, obtain filopodia number, filopodia length and filopodia tortuosity/straightness values from the traced filaments.

Table 2: Troubleshooting

Step	Problem	Possible reasons	Possible solution
1-2	Air bubbles in the Evans blue that can kill the animal (due to air embolism)	Air was aspirated into the syringe while filling it with EB. Air bubbles are difficult to see in the EB solution	Look under the light, very precisely and remove any air bubble from the syringe.
1-2	Animal does not become immediately blue	Evans blue was not injected intracardially	Pushing the needle too slowly into the animal results in failure to puncture the heart. If the needle is pushed too deep and the mouse does not get blue when starting the injection retract the needle slightly to re-enter the ventricle and inject the remaining EB. Alternatively, retract the needle completely and try once more. Always use for each puncturing attempt a new needle as it must be really sharp. Better solution: Inject a new animal because paracardial injection (failed injection) might disturb the animal's circulation, and thus could result in a falsely high portion of non-perfused capillaries.
1-2	Animal gets too blue (Evans blue diffuses into the brain parenchyma)	Too much Evans blue was injected	Animal has to be excluded Inject a new animal. Adjust the amount of Evans blue exactly to 6 µl/g body weight (rather a little bit less than too much)
16-17	During cutting of brain sections, the brain tissue crumbles	Temperature of knife and/or tissue block is too low	One day before cutting, put the frozen sections from -80°C to -20°C Increase the temperature of the knife and of the tissue block
16-17	During cutting of brain sections, sections do not deroll in the PB	Temperature of knife and/or of tissue block is too high	if sections do not deroll, put sections in 0.1M PBS onto a shaker until they deroll at room temperature. Decrease the temperature of the knife and of the tissue block
7-8 19-26	Weak Evans blue staining Poor antigeneicity	Suboptimal fixation	Use freshly prepared fixative solutions (4% (wt/vol) formaldehyde (FA) solution + 0.025%/0.05% glutaraldehyde (GA) solution) After Evans blue perfusion, fix the brains in 4% FA + 0.025% GA or in or in % FA + 0.05% GA over night at 4°C

			Cryoprotect the brains for 2-3 days in 30% sucrose at 4°C optimize antibody concentration; test alternative antibodies
8, 20	Endothelial tip cells (and/or filopodia) not clearly visible	Fixation or postfixation too long	Exclude the section from the analysis
23-26	Weak antibody staining	Suboptimal antibody concentration	Optimize the concentrations for the first- and second antibodies; optionally, use fresh antibody batches or test antibodies from other manufacturers.
		Insufficient tissue penetration of antibodies	Adapt the incubation time of the antibodies; use higher amounts of Triton-X
27-28	Air bubbles in mounted sections	Trapping of air bubbles during coverslipping	Carefully lower the coverslip onto the section to avoid trapping of air bubbles
26, 28	High background staining	Insufficient washing after antibody incubation	Increase the frequency (not the duration) of the PBS-washes after and between antibody incubation steps

ANTICIPATED RESULTS

With the technique described here, perfused blood vessels, the non-perfused segments of new vessels (e.g. vessel sprouts), the total vascular network, the number of endothelial tip cells as well as the number of filopodia per tip cell can be quantitatively assessed in the postnatal mouse brain. Blood vessels and endothelial tip cells extending numerous (Fig. 6q,t) filopodia were visualized in different brain regions of postnatal day 8 (P8) mouse brain sections using IB4 staining (Fig. 3b-f). Endothelial tip cells were found in various brain regions including cortex, hippocampus and corpus callosum (Fig. 3c-f), indicating active sprouting angiogenesis at this stage of mouse development. IB4 also labels microglia/macrophages (Fig. 3g-j), as described earlier[54,55]. Therefore we recommend a double labeling with IB4 and a microglial/macrophage marker such as Iba1 to distinguish $IB4^+/Iba1^-$ endothelial cells from $IB4^+/Iba1^+$ microglia/macrophages (Fig. 3g-j). In our hands, this staining protocol identifies tip cells better than the suggested tip cell markers VEGFR2, VEGFR3 or Dll4[24,63,64] (Supplementary Fig. S2a-l). One reason may be that Dll4, VEGFR2, and VEGFR3 are internalized and thus less abundant at the cell surface, as previously shown for VEGFR2[82-86] and for VEGFR3[87]. Moreover, as there is still no specific endothelial tip cell marker, morphological features are crucially needed in order to identify this specific cell type appropriately.

Functional, perfused blood vessels can be best visualized with a marker that is injected into the circulation of an intact, living animal. To this end, we used Evans blue (EB) that labels the vascular lumen of actively, *in vivo* perfused blood vessels. Thus, $EB^+/IB4^+$- perfused vessels can be distinguished from $IB4^+$ but EB^- forming blood vessels that are not yet functional/perfused (Fig. 4a-c, Fig. 6, Supplementary Fig. S1) and from endothelial tip cells (Fig. 4d-f, Fig. 6, Supplementary Fig. S1). The basement membrane - visualized by Laminin (LN) – was present around perfused blood vessels but only partially at the tip cell body (Fig. 4g-k,m, Fig. 6l,p), allowing further differentiation of various steps in blood vessel maturation.

Endothelial tip filopodia were quantified by filament tracing in Imaris (Fig. 4d-f,l, Fig. 6h,q-t Box 1). Vessel parameters such as vessel volume fraction, vascular length and number of branch points of $EB^+/IB4^+$ perfused vessels and $EB^-/IB4^+$ sprouting vessels as well as the tissue volume density of $IB4^+$ endothelial tip cells can be quantified using a stereological method adapted from[36,41] (Fig. 5a-n, Box 2). For quantitative assessment of angiogenic features such as vessel volume fraction, vessel length, vascular branch points and endothelial tip cells, we recommend to track all counted structures using markers provided by all stereological software packages (Fig.5d-i, Box 2). Examples of quantification of the aforementioned vessel parameters in the postnatal mouse cortex are displayed in Fig. 5j-n. Stereological analysis revealed that 3.86% of the total volume of the postnatal mouse brain tissue was occupied by vessel structures (perfused or non-perfused), which is in accordance with previous findings[88,89]. Of the total vessel tissue volume, 3.58% (92.75% of the total vessel volume) were occupied by perfused vessels and 0.28% (7.25% of the total vessel volume) by non-perfused vessels (Fig. 5j). This corresponds to a total of 2782 capillaries (capillary segments from branchpoint to branchpoint) per mm^3 of postnatal mouse brain tissue of which 2034 capillaries/mm^3 were perfused and 748 capillaries/mm^3 were non-perfused, respectively. In one mm^3 of postnatal mouse brain tissue, the total length of vessel structures was 904 mm, of which 830 mm were perfused and 74 mm were not perfused (Fig. 5k). Furthermore, our analysis revealed 4918 branchpoints of valence 3 (3 vessel branches emanating from the vessel branch point) per mm^3 (3635 perfused and 1283 non-perfused), 321 branchpoints of valence 4 (4 vessel branches emanating from the vessel branchpoint) per mm^3 (214 perfused and 107 non-perfused) (Fig. 5l,m) and 2028 endothelial tip cells per mm^3 (Fig. 5n).

Endothelial tip cell filopodia can only be recognized in the IB4 but not in the EB channel (Fig. 5i lower row). In addition to these measured values, further values such as the number of capillaries (total: 2782 capillaries/mm^3, perfused: 2034 capillaries/mm^3, non-perfused: 748

capillaries/mm^3), the average capillary length (325 µm), average capillary radius (2.7 µm) and the average maximal perfusion distance (19.6 µm) can be derived (Fig. 5g lower row). Given the high angiogenic activity in the postnatal rodent brain[11], it is obvious that the precise values of the aforementioned parameters will vary depending on the exact developmental stage of the animal.

The combination of EB perfusion and IB4- and LN immunofluorescence can be used to further characterize endothelial tip cells (Fig. 6). We observed two groups of filopodia-extending endothelial cells: the first group at the leading edge of the vascular sprout (extending numerous (around 23 per cell), longer filopodia; classified as "endothelial tip cells"), and the second group along the body of the vessel sprout (extending fewer (around 8 per cell), shorter filopodia; classified as "endothelial cells with filopodia") (Fig. 6a-p,q,r,t). Whereas the number of filopodia per cell and the filopodia length varied significantly between these two groups, the filopodia straightness did not (Fig. 6s,t). These values might vary in different experimental settings and thus correlate with the angiogenic activity of the investigated tissue[24]. However, it is important to state that these specifications of single endothelial cells at a given time point may rapidly change as the tip vs. stalk cell phenotypes were shown to be transient[66]. Nevertheless, we feel that the filopodia density per tip cell as well as the average length of the filopodia obtained from a larger cell population might be helpful readouts for better understanding angiogenesis in various biological settings.

In the CNS, the neurovascular unit involves multiple cell types such as astrocytes, pericytes, neurons and microglia that are recruited subsequently to the forming vessels[7] and are necessary for the proper function of the CNS vasculature[8,90,91]. Our protocol allows simultaneous visualization and analysis of these perivascular cells (Supplementary Fig. S3 and Table 2 antibodies). For example, GFAP$^+$ astrocytes form astrocytic endfeet on the basement membrane enclosing both, the endothelium and the pericyte (Supplementary Fig. S3a-d). At P8, retracting radial glia is also GFAP$^+$ (Supplementary Fig. S3a,b,d), in

accordance with previous reports[12]. PDGFRβ^{+} pericytes (Supplementary Fig. S3e-h) stabilize the endothelium and the two cell types are embedded in a common basement membrane (Supplementary Fig. S3i-l). Neuronal cell protrusions, for instance Nf160^{+} axons in the corpus callosum, can also be visualized (Supplementary Fig. S3m-p). Of note, as virtually any antibody of interest can be used in our protocol, it is for example also possible to further distinguish arteries/arterioles from veins/venules although we do not describe how to do this.

Table 3: Examples of markers and antibodies for endothelial cells, perfused vessels and perivascular cell types of the neurovascular unit

Cell type/ Vascular structure	**Marker/Primary antibody**	**Secondary antibody/ Detection system**	**Important remarks**
Endothelial phalanx -stalk, and -tip cell (filopodia)	Biotinylated IB4 (Sigma, L 2140), diluted 1:50 in $CaCl_2$-containing buffer	Streptavidin-Cy3 (green, Ex: 550nm; Em: 570nm), Streptadivin-Alexa Fluor 543 (red), Strepdavidin-Dye-light 647 (red), all 1:500 in $CaCl_2$-containing buffer	Binds to sugar residues on the endothelium Marks established, perfused as well as newly forming blood vessels including endothelial tip cell filopodia Also marks microglia, macrophages
	Rabbit anti-VEGFR2 antibody (Cell Signaling, cat. no. 2479), diluted 1:1,000 in $CaCl_2$-containing buffer Goat anti-VEGFR3 antibody (R&D Systems, cat. no. AF743) diluted 1:1,000 in $CaCl_2$-containing buffer Rabbit anti-Dll4 antibody (R&D Systems, cat. no. MAB1389) diluted 1:1,000 in $CaCl_2$-containing buffer		Suggested endothelial tip cell markers that bind to surface receptors on the endothelium. All three markers preferentially label endothelial tip cell bodies but less intensively their filopodia. Moreover, they also label endothelial stalk- and phalanx cells. Thus, these markers label perfused as well as newly forming blood vessels
Microglia	Anti-rabbit Iba1 Wako, Code NO. 019-19741), diluted 1 :200 in $CaCl_2$-containing buffer	According to the combination with other markers/antibodies	Binds to sugar residues Marks non-activated/activated microglia
Perfused vessels	Evans blue (Dye content ≥ 75%, Sigma, E2129), diluted in 0.9% NaCl	Autofluorescent (far red, Ex.: 633 nm; Em.: 640 – 700 nm)	Binds to serum albumin Marks established, perfused blood vessels but newly forming blood vessels and endothelial tip cell (filopodia)
Astrocytes	Rabbit-anti GFAP (Dako, Z 0334), diluted 1 :1000 in	According to the combination with other	Binds to Glial fibrillary acidic protein (GFAP), which is the principal

	$CaCl_2$-containing buffer	markers/antibodies	intermediate filament of mature astrocytes
Pericytes	Rat-anti-mouse PDGFRβ (CD140b) (eBioscience, 12 1402), diluted 1 :200 in $CaCl_2$-containing buffer	According to the combination with other markers/antibodies	Binds to CD140b molecule, the β chain of the platelet derived growth factor receptor (PDGF receptor)
Neurons	Rat-anti-mouse Nf160 Zymed,13-0700), diluted 1: 250 in $CaCl_2$-containing buffer	According to the combination with other markers/antibodies	Binds to neurofilaments (Nf) in neurons

Ex. : Excitation ; Em. : Emission

ACKNOWLEDGMENTS

We thank Lutz Slomianka for help with stereological analysis and Andrin Wacker for critical reading of the manuscript. T.W. was supported by an MD-PhD fellowship of the Swiss National Science Foundation, by the Olga Mayenfisch Foundation, the Hartmann Muller Foundation, the EMDO Foundation, and by the MD-PhD student allowance of the Swiss Society for Microvascular Research (SSMVR). J.V. was supported by the Swiss National Science Foundation (310000 120321/1).

All the animal experiments were conducted in J.V.'s laboratory and were approved by the Veterinary office of the Canton of Zurich. The histological studies were performed in MES's laboratory. Microscopy image acquisition and analysis was performed in MES's Laboratory and at the Center for Microscopy and Image Analysis, University of Zurich.

AUTHOR CONTRIBUTIONS

T.W. and J.V. designed the experiments. T.W., O.W., and J.V. conducted the experiments. T.W. and J.M.M. analyzed the data. J.V. and M.E.S. supervised the experiments in their respective labs. T.W. and J.V. wrote the manuscript. D.B. helped with the endothelial tip cell marker experiments and gave critical inputs to the manuscript. H.G., S.P.H. and L.R. gave critical inputs to the manuscript. All authors read and approved the final manuscript.

COMPETING FINANCIAL INTERESTS

The authors declare no competing financial interests.

FIGURE LEGENDS

Figure 1 Flow chart, summary, and time frame of the protocol

The different sections of the protocol are indicated in color-coded boxes. White boxes indicate preparation steps, green boxes describe experimental steps, blue boxes indicate analysis steps and brown boxes describe quality control steps. Black arrows indicate the order in which the different steps of the protocol are performed. The left side provides a time scale.

Figure 2 Intracardial Evans blue injection and brain dissection

a,b Angles (**a,b**) and site (white arrowheads (**b,c**), ~1-2 mm below the horizontal line connecting both armpits; ~1-2 mm on the right side of the midline) for intracardial Evans blue injection in a P8 mouse pup (see also Supplementary Video 1). **c** Comparison between an animal before injection (left side) and after Evans-injection (right side). Successful perfusion is indicated by a bluish aspect of the animal, which can be well observed at the paws (right side, arrows), snout or tail. White arrowhead marks the injection site. **d-f** Dissection of a P8 mouse brain (see also Supplementary Video 2). Position and stabilize the head between two fingers in a convenient orientation (**d**). Open the skull using a fine spring scissor starting at the foramen magnum (arrow in **d**) and cut the scull on both sides to the rostral end. Then lift up the scull (arrow in **e**) with the scissor or a forceps and verify that the meninges (including tentorium cerebelli) are removed completely. The brain is then carefully lifted caudally with a fine forceps that is also used to cut the brain nerves (e.g the trigeminal nerves, marked with arrows in **f**). **g** Comparison of a dissected Evans blue-injected P8 mouse brain (blue, top) and a non-injected P8 mouse brain (light red, bottom). The bluish appearance of the Evans blue injected mouse brain serves as a quality control (see Fig. 1). Dashed lines indicate planes where to cut the brain tissue. **h** Coronal slices of an Evans blue injected P8 mouse brain after cutting as indicated in **g**. Scale bars: 5 mm (**g,h**).

Figure 3 Visualization of blood vessel endothelium and endothelial tip cells in the postnatal mouse brain at P8

a Schematic representation of postnatal mouse brain vascularization (red) on coronal brain sections. The selection of the brain regions analyzed here has been done on coronal sections in the structures selected using the Developing Mouse Allen Brain Atlas. A corresponding immunofluorescence image of the boxed area taken at low magnification is shown in **b**. **b** Overview of a 40 µm P8 coronal mouse brain section labeled with biotinylated IB4 to visualize vascular endothelial cells (red). Cell nuclei (DAPI, blue). **c-f** $IB4^+$ endothelial tip cells extending multiple filopodia (red) in layer V (**c**) and in layer VI could be found in gray matter structures such as the cingulate cortex (**c,d**) or CA1 (**e**) of the hippocampus as well as in white matter structures such as the corpus callosum (**f**). Cell nuclei were counterstained with DAPI (blue). **q-j** Iba1 (green) and IB4 staining (red) in the P8 mouse cortex. Boxed area is enlarged in **h-j**. IB4 labels endothelial cells (including endothelial tip cells) but also microglia (**g-i**). $IB4^+$ but $Iba1^-$ structures can be identified as endothelial cells (**g,h**) whereas $IB4^+$ and $Iba1^+$ structures are microglia (**g-j**). Cell nuclei were counterstained with DAPI (blue).

Scale bars: 500 µm (**b**) ; 50 µm (**g**), 10 µm (**c-f, h-j**)

SS = Sagittal sulcus; Ctx = Cortex ; CC = Corpus Callosum; CA 1 = Cornu Ammonis 1; CA 3 = Cornu Ammonis 3; DG = Dentate Gyrus.

Figure 4 Discrimination between perfused blood vessels and newly forming sprouting blood vessels and endothelial tip cells in the P8 mouse cortex

a-m Perfused and non-perfused blood vessels in P8 WT mouse cortex. **a-c** Confocal images of an EB-perfused P8 WT mouse cortex stained for IB4 to visualize blood vessel endothelial cells. IB4 (red) labels the endothelium of the entire vascular tree (**a,c**). Functional-perfused blood vessels are labeled with EB (**b**) and are $EB^+/IB4^+$ (**c**). In contrast, not yet perfused, newly forming blood vessels are $EB^-/IB4^+$ (**c**). The boxed area is enlarged in **d-f**. Arrowheads in (**a,b**) point to $IB4^+$ but EB^- vessels that are not perfused. .**d** Perfused vessels and vascular sprouts including endothelial tip cells are shown. White solid arrowheads indicate $IB4^+$ but EB^- endothelial tip cells extending multiple filopodia, thus, non-perfused not yet functional vascular structures. White arrow indicates a newly forming vascular sprout with its endothelial tip cell emanating from a functional $EB^+/IB4^+$ perfused blood vessel. White open arrowheads show $EB^+/IB4^+$ perfused blood vessels including endothelial stalk- and phalanx cells. **e** 3D rendering of the image shown in (**d**) generated with Imaris software (see Box 1) to separate blood vessels from microglia. IB4-labeled blood vessel structures are coded in yellow, EB-labeled blood vessel structures are coded in blue and microglia is displayed in red. (**f**) 3D rendering of data in (**e**) showing reconstructed IB4-labeled vessels using isosurfaces with subtracted background (no microglia visible). **g-k** 3D confocal stacks of a newly forming blood vessel that sprouts from a pre-existing blood vessel. IB4 (red) labels the entire vascular network including endothelial tip cell filopodia, Laminin (LN, green) marks the vascular basement membrane and EB (cyan) highlights the perfused vessel parts. LN^+ structures (green) enclose EB^+ vessel parts (cyan) and LN^+ structures indicate at least partially matured vessel structures. DAPI-stained cell nuclei (blue). **l** Reconstruction of the vascular sprout and the endothelial tip cell displayed in **g-k** by Imaris software using isosurfaces (displayed in green) and filopodia tracing (displayed in red) (see Box 1). **m** Scheme of the different structures of sprouting angiogenesis in the postnatal mouse brain and illustration how these

can be distinguished with our method. Sprouting blood vessels emanating from an established blood vessel are led by endothelial tip cells sensing the CNS-microenvironment for attractive and repulsive guidance cues using finger-like filopodia, thereby steering the growing blood vessels. Perfused blood vessels are $EB^{+}/IB4^{+}$, vascular sprouts are $EB^{+}/IB4^{+}$ or $EB^{-}/IB4^{+}$. The endothelial tip cell body and its filopodial tree are $EB^{-}/IB4^{+}$. LN indicates the vascular basement membrane.

Scale bars: 100 µm (**a-c**) ; 50 µm (**d-f**) ; 10 µm (**g-l**)

Figure 5 Stereological analysis of the vascular network in the P8 mouse cortex

a-c Confocal images of a P8 mouse cortical brain section. Blood vessel endothelial cells are visualized using IB4 (**a,c**) and perfused vessels are highlighted by EB (**b,c**). Regions of interest (ROI) are indicated (white boxes). **d-f** Different probes in are used to quantify various aspects of the 3D vascular network, e.g. the area fractionator (displayed as white point grid squares) to quantify the vessel volume fraction (**d**), spaceballs (intersections are displayed as green dots) to quantify the vascular length (**e**) and the optical fractionator (counts are displayed as different symbols) to analyze the number of branchpoints and endothelial tip cells (**f**). These analyses are done for both channels, IB4 and EB (only IB4 is shown for the overviews (**d-f**)). The boxed areas are enlarged in (**g-i**). **g-i** Examples of how to analyze different parameters of the 3D vascular network in the P8 mouse cortex. Multiple point grid squares (100 µm x 100 µm) (see box 2) are randomly superimposed on the region of interest (ROI) within confocal images to analyze the vessel volume fraction (**g**). Grid points overlaying vessel structures are counted. White dots mark $EB^+/IB4^+$ perfused vessels whereas green dots mark $EB^-/IB4^+$ non-perfused forming blood vessels (**g**). Spaceballs (hemispheres) (see box 2) with a maximal diameter of 40 µm are randomly placed on the ROI within confocal images to analyze the vessel length. Intersections of vessel structures with the spaceball-surface are counted in the IB4- (left side) and in the EB channel (right side) and are marked by green dots (**h**). Note that intersections are only counted if they appear in focus (upper row), but not if they are out of focus (lower row) (**h**). Squares of 100 µm x 100 µm (for branchpoints, upper row) or of 150 µm x 150 µm (for endothelial tip cells, lower row) are randomly placed on the ROI within confocal images to analyze the number of branchpoints (upper row) or the number of endothelial tip cells (lower row). Branchpoints or endothelial tip cells within these frames are counted. Branchpoints or endothelial tip cells falling onto the green sides of the square (right and upper) are taken into account whereas branchpoints or endothelial tip cells falling onto the red sides of the square (left and lower) are not counted

(**h**). Branchpoints are analyzed in the IB4- (upper line, left side) and in the EB channel (upper line, right side). Branchpoints of valence 3 (3 vessel branches emanating from the vessel branchpoint) are marked with green stars and branchpoints of valence 4 (4 vessel branches emanating from the vessel branchpoint) are marked with white stars. Endothelial tip cells are analyzed in the IB4 channel (lower line, left side; marked with a double yellow circle) but do not appear in the EB channel (lower line, right side). Table shown in (**g**) summarizes measured and derived values for characterization of the vascular network. **j-n** Values of the different vessel parameters in the P8 mouse brain cortex as described above. Vessel volume fraction of perfused-, non-perfused- and total vessels (**j**). In a P8 mouse brain cortex, ~3.86% of the tissue is occupied by vessel structures, from which ~92.75% are perfused and ~7.25% are non-perfused (**j**). Length of perfused-, non-perfused- and total vessels (**k**). Number of branchpoints of valence 3 (**l**) and of valence 4 (**m**) of perfused-, non-perfused- and total vessels (**l,m**). Number of cortical endothelial tip cells (**n**). There are 2028 endothelial tip cells in a mm^3 P8 mouse brain cortex.

Scale bars: 200 μm (**a-f**), 50 μm (**g-i**).

Figure 6 Characterization of endothelial tip cells in the postnatal mouse brain at P8

a,b Endothelial tip cell in the P8 mouse cortex, visualized by IB4-labeling (**a**). Note the well-defined cell body, the numerous, finger-like filopodia extending from the tip cell body and the absence of EB labeling (**a**). Next to the endothelial tip cell, a $EB^+/IB4^+$ perfused blood vessel is visible (**b**). Cell nuclei (DAPI, blue). **c,d** Endothelial cell extending filopodia (**c**) on both sides of an $EB^+/IB4^+$ perfused blood vessel (**d**) in the P8 mouse cortex, visualized by $IB4^+$. This endothelial cell extends few filopodia that are oriented ~90° to the axis of the blood vessel from which they emanate. Note the absence of a well-defined cell body (**c**). Cell nuclei (DAPI, blue). **e-g** Vascular sprout in the P8 mouse cortex. Two tip cells at the forefront of the vascular sprout and an endothelial cell extending filopodia in the body of the vascular sprout are shown. $EB^-/IB4^+$ filopodia and $EB^+/IB4^+$ perfused blood vessel are displayed. **h** Endothelial tip cells and endothelial cells with filopodia can be visualized using IMARIS software. Isosurfaces are used to visualize the body of the vessel sprout (green) and filopodia are traced using the filament tracer module in IMARIS (red) (see Box 1). Different structures of the vascular sprout are labeled. **i-k** Two $IB4^+$ Endothelial tip cells extending numerous filopodia at the forefront of a vascular sprout in the P8 mouse cortex. Note that vascular sprout bodies are well developed and perfused, as highlighted by EB (**i,j,k**). The filopodial tree is well established ("finger- or hand-like") and filopodia extend mainly in the axis of the EB-perfused vascular sprout body (**i,j,k**). **l** Part of vascular sprout behind the tip cell with a well-established, LN^+ vascular basement membrane surrounding the EB^+ perfused vessel lumen. **m-p** $IB4^+$ endothelial cell extending few filopodia. A sprout body in the axis of the filopodia has not developed yet (**m,n,o**) and its filopodial tree is less well established with filopodia oriented mainly ~90° to the axis of the existing, EB-perfused vascular sprout (**m,n,o**). **p** Part of vascular sprout behind the tip cell. Note LN^+ vascular basement membrane surrounding the EB^+ perfused vessel lumen. **q-s** Comparison of different quantitative filopodia parameters between endothelial tip cells and endothelial cells extending filopodia.

The filopodia number per tip cell is ~3 times higher for endothelial tip cells as compared to endothelial cells extending filopodia (**q**). Moreover, endothelial tip cells extend 1.5 times longer filopodia than endothelial cells with filopodia (**r**). No major difference in filopodia straightness was found between endothelial tip cells and endothelial cells extending filopodia (**s**). **t** Table summarizing different typical features of tip cells and of endothelial cells extending filopodia. All data are shown as mean ± s.e.m. (n = 7-10). *$P < 0.05$, **$P < 0.01$, ***$P < 0.001$.

Scale bars: 10 µm (**a-d**); 20 µm (**e-g**); 10 µm (**h**), 10 µm (**i-k**) ; 5 µm (**l**); 5 µm (**m-p**).

REFERENCES

1 Carmeliet, P. & Jain, R. K. Molecular mechanisms and clinical applications of angiogenesis. *Nature* **473**, 298-307, doi:10.1038/nature10144 (2011).

2 Potente, M., Gerhardt, H. & Carmeliet, P. Basic and therapeutic aspects of angiogenesis. *Cell* **146**, 873-887, doi:10.1016/j.cell.2011.08.039 (2011).

3 Jain, R. K. & Carmeliet, P. SnapShot: Tumor angiogenesis. *Cell* **149**, 1408-1408 e1401, doi:10.1016/j.cell.2012.05.025 (2012).

4 Burri, P. H., Hlushchuk, R. & Djonov, V. Intussusceptive angiogenesis: its emergence, its characteristics, and its significance. *Dev Dyn* **231**, 474-488, doi:10.1002/dvdy.20184 (2004).

5 Makanya, A. N., Hlushchuk, R. & Djonov, V. G. Intussusceptive angiogenesis and its role in vascular morphogenesis, patterning, and remodeling. *Angiogenesis* **12**, 113-123, doi:10.1007/s10456-009-9129-5 (2009).

6 Herbert, S. P. & Stainier, D. Y. Molecular control of endothelial cell behaviour during blood vessel morphogenesis. *Nat Rev Mol Cell Biol* **12**, 551-564, doi:10.1038/nrm3176 (2011).

7 Mancuso, M. R., Kuhnert, F. & Kuo, C. J. Developmental angiogenesis of the central nervous system. *Lymphat Res Biol* **6**, 173-180, doi:10.1089/lrb.2008.1014 (2008).

8 Quaegebeur, A., Lange, C. & Carmeliet, P. The neurovascular link in health and disease: molecular mechanisms and therapeutic implications. *Neuron* **71**, 406-424, doi:10.1016/j.neuron.2011.07.013 (2011).

9 Fantin, A., Vieira, J. M., Plein, A., Maden, C. H. & Ruhrberg, C. The embryonic mouse hindbrain as a qualitative and quantitative model for studying the molecular and cellular mechanisms of angiogenesis. *Nat Protoc* **8**, 418-429 (2013).

10 Daneman, R., Zhou, L., Kebede, A. A. & Barres, B. A. Pericytes are required for blood-brain barrier integrity during embryogenesis. *Nature* **468**, 562-566, doi:10.1038/nature09513 (2010).

11 Zeller, K., Vogel, J. & Kuschinsky, W. Postnatal distribution of Glut1 glucose transporter and relative capillary density in blood-brain barrier structures and circumventricular organs during development. *Brain Res Dev Brain Res* **91**, 200-208 (1996).

12 Walchli, T. *et al.* Nogo-A is a negative regulator of CNS angiogenesis. *Proc Natl Acad Sci U S A* **110**, E1943-1952, doi:10.1073/pnas.1216203110 (2013).

13 Geudens, I. & Gerhardt, H. Coordinating cell behaviour during blood vessel formation. *Development* **138**, 4569-4583, doi:10.1242/dev.062323 (2011).

14 Eilken, H. M. & Adams, R. H. Dynamics of endothelial cell behavior in sprouting angiogenesis. *Curr Opin Cell Biol* **22**, 617-625, doi:10.1016/j.ceb.2010.08.010 (2010).

15 Strilic, B. *et al.* The molecular basis of vascular lumen formation in the developing mouse aorta. *Dev Cell* **17**, 505-515, doi:10.1016/j.devcel.2009.08.011 (2009).

16 Lammert, E. & Axnick, J. Vascular lumen formation. *Cold Spring Harb Perspect Med* **2**, a006619, doi:10.1101/cshperspect.a006619 (2012).

17 Tung, J. J., Tattersall, I. W. & Kitajewski, J. Tips, Stalks, Tubes: Notch-Mediated Cell Fate Determination and Mechanisms of Tubulogenesis during Angiogenesis. *Cold Spring Harb Perspect Med* **2**, a006601, doi:10.1101/cshperspect.a006601 (2012).

18 Wacker, A. & Gerhardt, H. Endothelial development taking shape. *Curr Opin Cell Biol* **23**, 676-685, doi:10.1016/j.ceb.2011.10.002 (2011).

19 Mazzone, M. *et al.* Heterozygous deficiency of PHD2 restores tumor oxygenation and inhibits metastasis via endothelial normalization. *Cell* **136**, 839-851, doi:10.1016/j.cell.2009.01.020 (2009).

20 Pries, A. R., Secomb, T. W. & Gaehtgens, P. Structural adaptation and stability of microvascular networks: theory and simulations. *Am J Physiol* **275**, H349-360 (1998).
21 Zhang, L., Cooper-Kuhn, C. M., Nannmark, U., Blomgren, K. & Kuhn, H. G. Stimulatory effects of thyroid hormone on brain angiogenesis in vivo and in vitro. *J Cereb Blood Flow Metab* **30**, 323-335, doi:10.1038/jcbfm.2009.216 (2010).
22 Frahm, K. A., Nash, C. P. & Tobet, S. A. Endocan immunoreactivity in the mouse brain: method for identifying nonfunctional blood vessels. *J Immunol Methods* **398-399**, 27-32, doi:10.1016/j.jim.2013.09.005 (2013).
23 Lobov, I. B. *et al.* Delta-like ligand 4 (Dll4) is induced by VEGF as a negative regulator of angiogenic sprouting. *Proc Natl Acad Sci U S A* **104**, 3219-3224, doi:10.1073/pnas.0611206104 (2007).
24 Blanco, R. & Gerhardt, H. VEGF and Notch in tip and stalk cell selection. *Cold Spring Harb Perspect Med* **3**, a006569, doi:10.1101/cshperspect.a006569 (2013).
25 Phng, L. K. & Gerhardt, H. Angiogenesis: a team effort coordinated by notch. *Dev Cell* **16**, 196-208, doi:10.1016/j.devcel.2009.01.015 (2009).
26 Thurston, G., Noguera-Troise, I. & Yancopoulos, G. D. The Delta paradox: DLL4 blockade leads to more tumour vessels but less tumour growth. *Nat Rev Cancer* **7**, 327-331, doi:10.1038/nrc2130 (2007).
27 Yan, M. *et al.* Chronic DLL4 blockade induces vascular neoplasms. *Nature* **463**, E6-7, doi:10.1038/nature08751 (2010).
28 Noguera-Troise, I. *et al.* Blockade of Dll4 inhibits tumour growth by promoting non-productive angiogenesis. *Nature* **444**, 1032-1037, doi:10.1038/nature05355 (2006).
29 Ridgway, J. *et al.* Inhibition of Dll4 signalling inhibits tumour growth by deregulating angiogenesis. *Nature* **444**, 1083-1087, doi:10.1038/nature05313 (2006).
30 Noguera-Troise, I. *et al.* Blockade of Dll4 inhibits tumour growth by promoting non-productive angiogenesis. *Novartis Found Symp* **283**, 106-120; discussion 121-105, 238-141 (2007).
31 Gobel, U., Theilen, H. & Kuschinsky, W. Congruence of total and perfused capillary network in rat brains. *Circ Res* **66**, 271-281 (1990).
32 Gundersen, H. J. Stereology of arbitrary particles. A review of unbiased number and size estimators and the presentation of some new ones, in memory of William R. Thompson. *J Microsc* **143**, 3-45 (1986).
33 West, M. J. Basic Stereology for Biologists and Neuroscientists. *Cold Spring Harbor: Cold Spring Harbor Laboratory Press*, 206 pp (2012).
34 Gundersen, H. J. & Jensen, E. B. The efficiency of systematic sampling in stereology and its prediction. *J Microsc* **147**, 229-263 (1987).
35 Boyce, R. W., Dorph-Petersen, K. A., Lyck, L. & Gundersen, H. J. Design-based stereology: introduction to basic concepts and practical approaches for estimation of cell number. *Toxicol Pathol* **38**, 1011-1025, doi:10.1177/0192623310385140 (2010).
36 Mouton, P. R., Gokhale, A. M., Ward, N. L. & West, M. J. Stereological length estimation using spherical probes. *J Microsc* **206**, 54-64 (2002).
37 Gundersen, H. J. *et al.* Some new, simple and efficient stereological methods and their use in pathological research and diagnosis. *APMIS* **96**, 379-394 (1988).
38 Gundersen, H. J. *et al.* The new stereological tools: disector, fractionator, nucleator and point sampled intercepts and their use in pathological research and diagnosis. *APMIS* **96**, 857-881 (1988).
39 Schmitz, C. & Hof, P. R. Design-based stereology in neuroscience. *Neuroscience* **130**, 813-831, doi:10.1016/j.neuroscience.2004.08.050 (2005).
40 Howard, C. V. & Reed, M. G. Unbiased Stereology. Three-dimensional Measurements in Microscopy. *QTP Publications, Liverpool* (2010).

41 Lokkegaard, A., Nyengaard, J. R. & West, M. J. Stereological estimates of number and length of capillaries in subdivisions of the human hippocampal region. *Hippocampus* **11**, 726-740, doi:10.1002/hipo.1088 (2001).
42 Carmeliet, P. Angiogenesis in life, disease and medicine. *Nature* **438**, 932-936, doi:10.1038/nature04478 (2005).
43 Storkebaum, E., Quaegebeur, A., Vikkula, M. & Carmeliet, P. Cerebrovascular disorders: molecular insights and therapeutic opportunities. *Nat Neurosci* **14**, 1390-1397, doi:10.1038/nn.2947 (2011).
44 Pitulescu, M. E., Schmidt, I., Benedito, R. & Adams, R. H. Inducible gene targeting in the neonatal vasculature and analysis of retinal angiogenesis in mice. *Nat Protoc* **5**, 1518-1534, doi:10.1038/nprot.2010.113 (2010).
45 Connor, K. M. *et al.* Quantification of oxygen-induced retinopathy in the mouse: a model of vessel loss, vessel regrowth and pathological angiogenesis. *Nat Protoc* **4**, 1565-1573, doi:10.1038/nprot.2009.187 (2009).
46 Rawson R.A. The binding of T-1824 and structurally related diazo dyes by the plasma proteins *Am J Physiol* **138**, 708-717 (1943).
47 Weintraub, H. *et al.* Storage of glycoprotein in NCTR-Balb/C mouse. Lectin histochemistry, and biochemical studies. *Virchows Arch B Cell Pathol Incl Mol Pathol* **62**, 347-352 (1992).
48 DeGasperi, R. *et al.* Glycoprotein storage in Gaucher disease: lectin histochemistry and biochemical studies. *Lab Invest* **63**, 385-392 (1990).
49 Laitinen, L. Griffonia simplicifolia lectins bind specifically to endothelial cells and some epithelial cells in mouse tissues. *Histochem J* **19**, 225-234 (1987).
50 Laitinen, L., Virtanen, I. & Saxen, L. Changes in the glycosylation pattern during embryonic development of mouse kidney as revealed with lectin conjugates. *J Histochem Cytochem* **35**, 55-65 (1987).
51 Alroy, J., Goyal, V. & Warren, C. D. Lectin histochemistry of gangliosidosis. I. Neural tissue in four mammalian species. *Acta Neuropathol* **76**, 109-114 (1988).
52 Gerhardt, H. *et al.* Neuropilin-1 is required for endothelial tip cell guidance in the developing central nervous system. *Dev Dyn* **231**, 503-509, doi:10.1002/dvdy.20148 (2004).
53 Gerhardt, H. *et al.* VEGF guides angiogenic sprouting utilizing endothelial tip cell filopodia. *J Cell Biol* **161**, 1163-1177, doi:10.1083/jcb.200302047 (2003).
54 Sorokin, S. P. & Hoyt, R. F., Jr. Macrophage development: I. Rationale for using Griffonia simplicifolia isolectin B4 as a marker for the line. *Anat Rec* **232**, 520-526, doi:10.1002/ar.1092320409 (1992).
55 Sorokin, S. P., Hoyt, R. F., Jr., Blunt, D. G. & McNelly, N. A. Macrophage development: II. Early ontogeny of macrophage populations in brain, liver, and lungs of rat embryos as revealed by a lectin marker. *Anat Rec* **232**, 527-550, doi:10.1002/ar.1092320410 (1992).
56 Theilen, H., Schrock, H. & Kuschinsky, W. Capillary perfusion during incomplete forebrain ischemia and reperfusion in rat brain. *Am J Physiol* **265**, H642-648 (1993).
57 Sawamiphak, S., Ritter, M. & Acker-Palmer, A. Preparation of retinal explant cultures to study ex vivo tip endothelial cell responses. *Nat Protoc* **5**, 1659-1665, doi:10.1038/nprot.2010.130 (2010).
58 Gore, A. V., Monzo, K., Cha, Y. R., Pan, W. & Weinstein, B. M. Vascular development in the zebrafish. *Cold Spring Harb Perspect Med* **2**, a006684, doi:10.1101/cshperspect.a006684 (2012).
59 Ellertsdottir, E. *et al.* Developmental role of zebrafish protease-activated receptor 1 (PAR1) in the cardio-vascular system. *PLoS One* **7**, e42131, doi:10.1371/journal.pone.0042131 (2012).

60 Carmeliet, P., De Smet, F., Loges, S. & Mazzone, M. Branching morphogenesis and antiangiogenesis candidates: tip cells lead the way. *Nat Rev Clin Oncol* **6**, 315-326, doi:10.1038/nrclinonc.2009.64 (2009).
61 Hellstrom, M. *et al.* Dll4 signalling through Notch1 regulates formation of tip cells during angiogenesis. *Nature* **445**, 776-780, doi:10.1038/nature05571 (2007).
62 Tammela, T. *et al.* Blocking VEGFR-3 suppresses angiogenic sprouting and vascular network formation. *Nature* **454**, 656-660, doi:10.1038/nature07083 (2008).
63 Strasser, G. A., Kaminker, J. S. & Tessier-Lavigne, M. Microarray analysis of retinal endothelial tip cells identifies CXCR4 as a mediator of tip cell morphology and branching. *Blood* **115**, 5102-5110, doi:10.1182/blood-2009-07-230284 (2010).
64 del Toro, R. *et al.* Identification and functional analysis of endothelial tip cell-enriched genes. *Blood* **116**, 4025-4033, doi:10.1182/blood-2010-02-270819 (2010).
65 Siemerink, M. J. *et al.* CD34 marks angiogenic tip cells in human vascular endothelial cell cultures. *Angiogenesis* **15**, 151-163, doi:10.1007/s10456-011-9251-z (2012).
66 Jakobsson, L. *et al.* Endothelial cells dynamically compete for the tip cell position during angiogenic sprouting. *Nat Cell Biol* **12**, 943-953, doi:10.1038/ncb2103 (2010).
67 Vogel, J., Gehrig, M., Kuschinsky, W. & Marti, H. H. Massive inborn angiogenesis in the brain scarcely raises cerebral blood flow. *J Cereb Blood Flow Metab* **24**, 849-859, doi:10.1097/01.WCB.0000126564.89011.11 (2004).
68 Heinzer, S. *et al.* Novel three-dimensional analysis tool for vascular trees indicates complete micro-networks, not single capillaries, as the angiogenic endpoint in mice overexpressing human VEGF(165) in the brain. *Neuroimage* **39**, 1549-1558, doi:10.1016/j.neuroimage.2007.10.054 (2008).
69 Kienast, Y. *et al.* Real-time imaging reveals the single steps of brain metastasis formation. *Nat Med* **16**, 116-122, doi:10.1038/nm.2072 (2010).
70 Whiteus, C., Freitas, C. & Grutzendler, J. Perturbed neural activity disrupts cerebral angiogenesis during a postnatal critical period. *Nature* **505**, 407-411, doi:10.1038/nature12821 (2014).
71 Harb, R., Whiteus, C., Freitas, C. & Grutzendler, J. In vivo imaging of cerebral microvascular plasticity from birth to death. *J Cereb Blood Flow Metab* **33**, 146-156, doi:10.1038/jcbfm.2012.152 (2013).
72 Chappell, J. C., Wiley, D. M. & Bautch, V. L. Regulation of blood vessel sprouting. *Semin Cell Dev Biol* **22**, 1005-1011, doi:10.1016/j.semcdb.2011.10.006 (2011).
73 Chappell, J. C., Wiley, D. M. & Bautch, V. L. How blood vessel networks are made and measured. *Cells Tissues Organs* **195**, 94-107, doi:10.1159/000331398 (2012).
74 West, M. J., Slomianka, L. & Gundersen, H. J. Unbiased stereological estimation of the total number of neurons in thesubdivisions of the rat hippocampus using the optical fractionator. *Anat Rec* **231**, 482-497, doi:10.1002/ar.1092310411 (1991).
75 West, M. J. Introduction to stereology. *Cold Spring Harbor protocols* **2012**, doi:10.1101/pdb.top070623 (2012).
76 West, M. J. The precision of estimates in stereological analyses. *Cold Spring Harb Protoc* **2012**, 937-949, doi:10.1101/pdb.top071050 (2012).
77 West, M. J. Estimating object number in biological structures. *Cold Spring Harb Protoc* **2012**, 1049-1066, doi:10.1101/pdb.top071423 (2012).
78 West, M. J. Estimating volume in biological structures. *Cold Spring Harb Protoc* **2012**, 1129-1139, doi:10.1101/pdb.top071787 (2012).
79 West, M. J. Systematic versus random sampling in stereological studies. *Cold Spring Harb Protoc* **2012**, doi:10.1101/pdb.top071837 (2012).
80 Reed, M. G., Howard, C. V. & GS, D. E. Y. One-stop stereology: the estimation of 3D parameters using isotropic rulers. *J Microsc* **239**, 54-65, doi:10.1111/j.1365-2818.2009.03356.x (2010).

81 Howard, C. V. & Reed, M. G. Unbiased Stereology. *Oxford: BIOS Scientific Publischers*, 246pp (1998).
82 Sawamiphak, S. *et al.* Ephrin-B2 regulates VEGFR2 function in developmental and tumour angiogenesis. *Nature* **465**, 487-491, doi:10.1038/nature08995 (2010).
83 Gampel, A. *et al.* VEGF regulates the mobilization of VEGFR2/KDR from an intracellular endothelial storage compartment. *Blood* **108**, 2624-2631, doi:10.1182/blood-2005-12-007484 (2006).
84 Jopling, H. M., Howell, G. J., Gamper, N. & Ponnambalam, S. The VEGFR2 receptor tyrosine kinase undergoes constitutive endosome-to-plasma membrane recycling. *Biochem Biophys Res Commun* **410**, 170-176, doi:10.1016/j.bbrc.2011.04.093 (2011).
85 Nakayama, M. *et al.* Spatial regulation of VEGF receptor endocytosis in angiogenesis. *Nat Cell Biol* **15**, 249-260, doi:10.1038/ncb2679 (2013).
86 Gaengel, K. & Betsholtz, C. Endocytosis regulates VEGF signalling during angiogenesis. *Nat Cell Biol* **15**, 233-235, doi:10.1038/ncb2705 (2013).
87 Wang, Y. *et al.* Ephrin-B2 controls VEGF-induced angiogenesis and lymphangiogenesis. *Nature* **465**, 483-486, doi:10.1038/nature09002 (2010).
88 Kent, T. A. *et al.* Cerebral blood volume in a rat model of ischemia by MR imaging at 4.7 T. *AJNR Am J Neuroradiol* **10**, 335-338 (1989).
89 Lin, W., Paczynski, R. P., Kuppusamy, K., Hsu, C. Y. & Haacke, E. M. Quantitative measurements of regional cerebral blood volume using MRI in rats: effects of arterial carbon dioxide tension and mannitol. *Magn Reson Med* **38**, 420-428 (1997).
90 Ruhrberg, C. & Bautch, V. L. Neurovascular development and links to disease. *Cell Mol Life Sci* **70**, 1675-1684, doi:10.1007/s00018-013-1277-5 (2013).
91 Eichmann, A. & Thomas, J. L. Molecular parallels between neural and vascular development. *Cold Spring Harb Perspect Med* **3**, a006551, doi:10.1101/cshperspect.a006551 (2013).

SUPPLEMENTARY VIDEO LEGENDS

Supplementary Video 1 Intracardial Evans blue injection of a P8 mouse This video shows the different steps of intracardial Evans blue (EB) injection of a P8 mouse pub. All steps are precisely explained in the “PROCEDURE” part of this manuscript.

Supplementary Video 2 Brain dissection of a P8 mouse

This video shows the different steps of brain dissection of an Evans-blue (EB) injected P8 mouse pup. All steps are precisely explained in the “PROCEDURE” part of this manuscript.

Figure 1

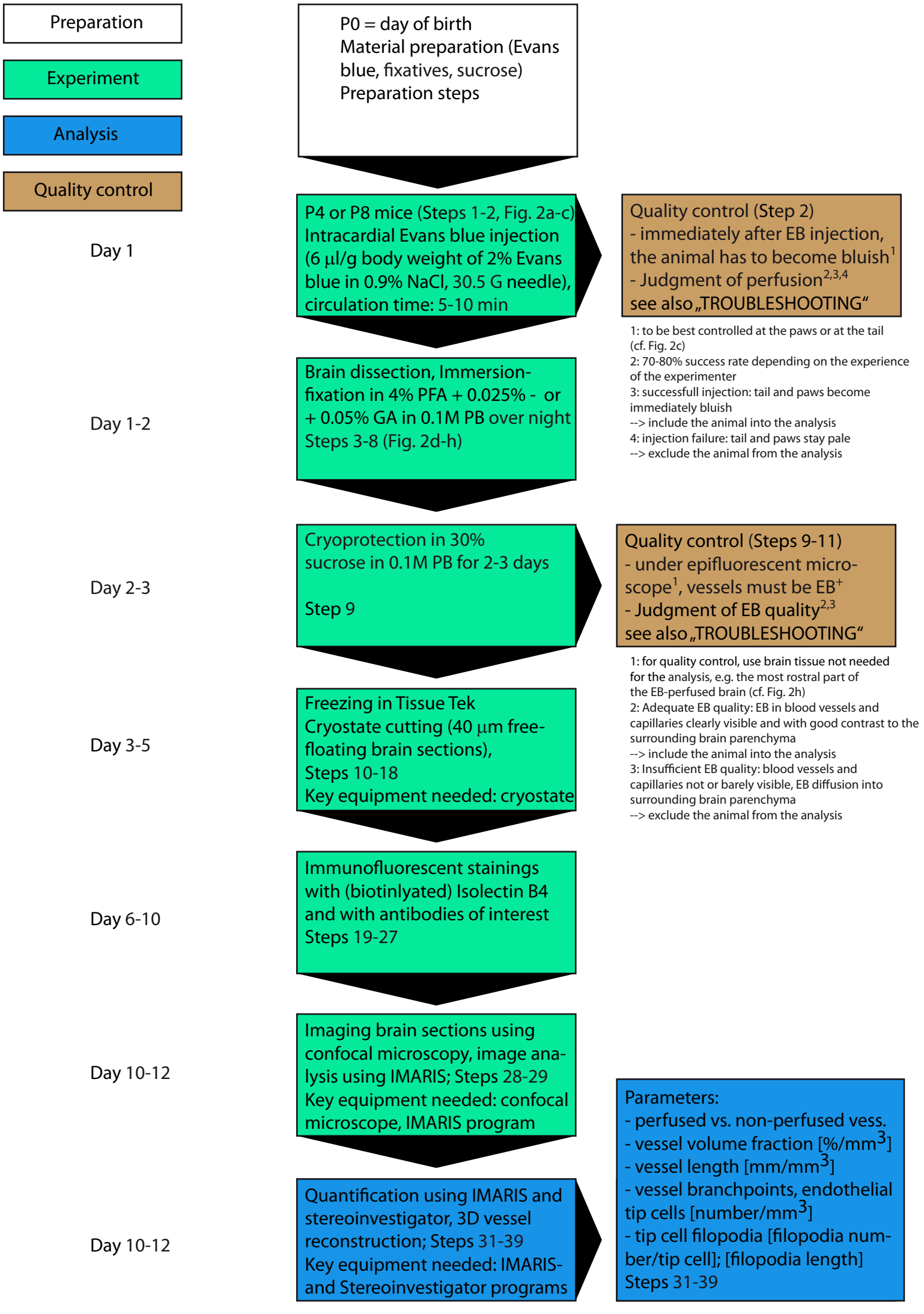
Preparation
Experiment
Analysis
Quality control
P0 = day of birth
Material preparation (Evans blue, fixatives, sucrose)
Preparation steps
Day 1
P4 or P8 mice (Steps 1-2, Fig. 2a-c)
Intracardial Evans blue injection (6 µl/g body weight of 2% Evans blue in 0.9% NaCl, 30.5 G needle), circulation time: 5-10 min
Quality control (Step 2)
- immediately after EB injection, the animal has to become bluish[1]
- Judgment of perfusion[2,3,4]
see also „TROUBLESHOOTING“
1: to be best controlled at the paws or at the tail (cf. Fig. 2c)
2: 70-80% success rate depending on the experience of the experimenter
3: successfull injection: tail and paws become immediately bluish
--> include the animal into the analysis
4: injection failure: tail and paws stay pale
--> exclude the animal from the analysis
Day 1-2
Brain dissection, Immersion-fixation in 4% PFA + 0.025% - or + 0.05% GA in 0.1M PB over night
Steps 3-8 (Fig. 2d-h)
Day 2-3
Cryoprotection in 30% sucrose in 0.1M PB for 2-3 days
Step 9
Quality control (Steps 9-11)
- under epifluorescent microscope[1], vessels must be EB+
- Judgment of EB quality[2,3]
see also „TROUBLESHOOTING“
1: for quality control, use brain tissue not needed for the analysis, e.g. the most rostral part of the EB-perfused brain (cf. Fig. 2h)
2: Adequate EB quality: EB in blood vessels and capillaries clearly visible and with good contrast to the surrounding brain parenchyma
--> include the animal into the analysis
3: Insufficient EB quality: blood vessels and capillaries not or barely visible, EB diffusion into surrounding brain parenchyma
--> exclude the animal from the analysis
Day 3-5
Freezing in Tissue Tek
Cryostate cutting (40 µm free-floating brain sections),
Steps 10-18
Key equipment needed: cryostate
Day 6-10
Immunofluorescent stainings with (biotinlyated) Isolectin B4 and with antibodies of interest
Steps 19-27
Day 10-12
Imaging brain sections using confocal microscopy, image analysis using IMARIS; Steps 28-29
Key equipment needed: confocal microscope, IMARIS program
Day 10-12
Quantification using IMARIS and stereoinvestigator, 3D vessel reconstruction; Steps 31-39
Key equipment needed: IMARIS- and Stereoinvestigator programs
Parameters:
- perfused vs. non-perfused vess.
- vessel volume fraction [%/mm3]
- vessel length [mm/mm3]
- vessel branchpoints, endothelial tip cells [number/mm3]
- tip cell filopodia [filopodia number/tip cell]; [filopodia length]
Steps 31-39

Figure 2

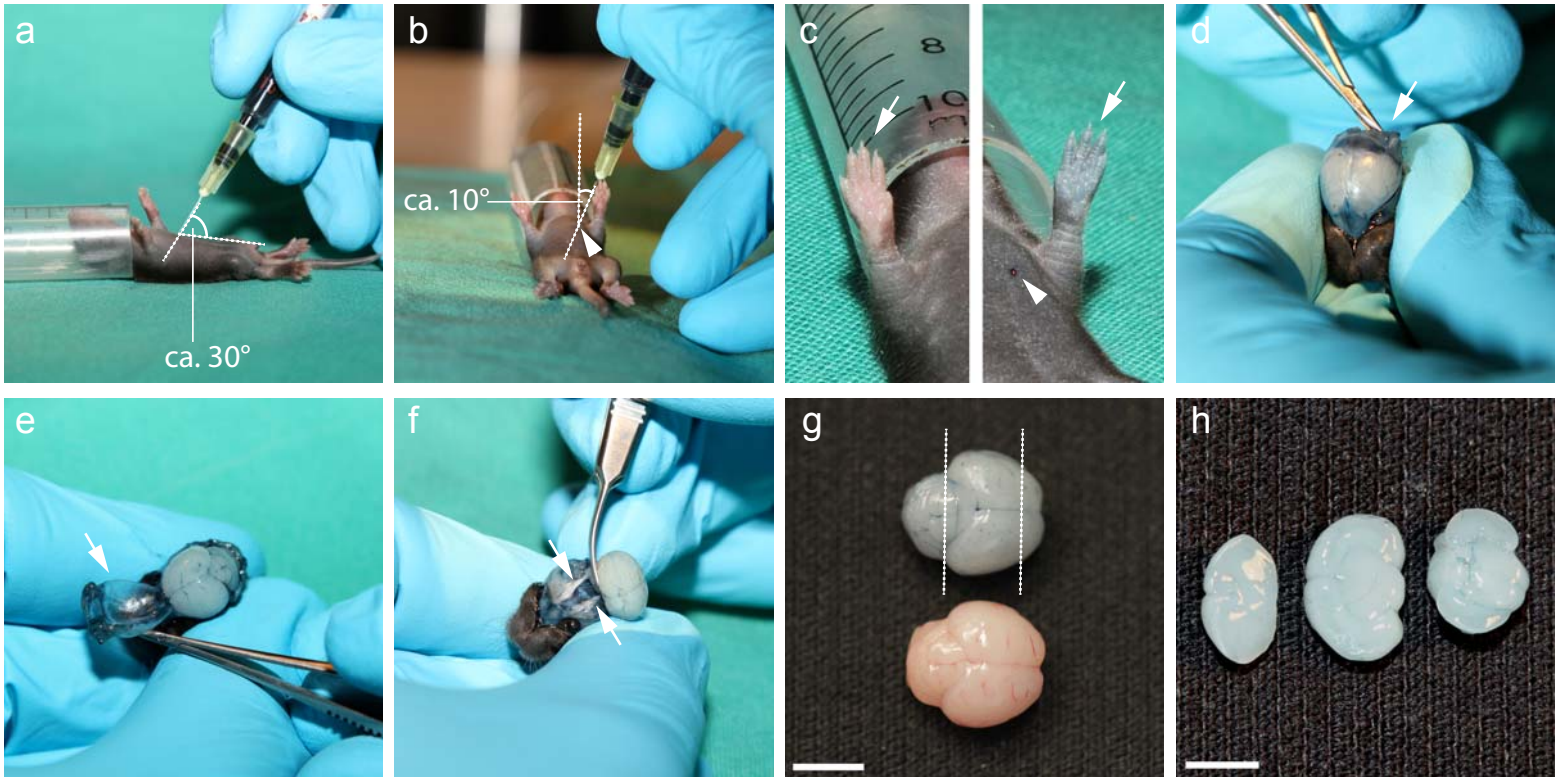

Figure 3

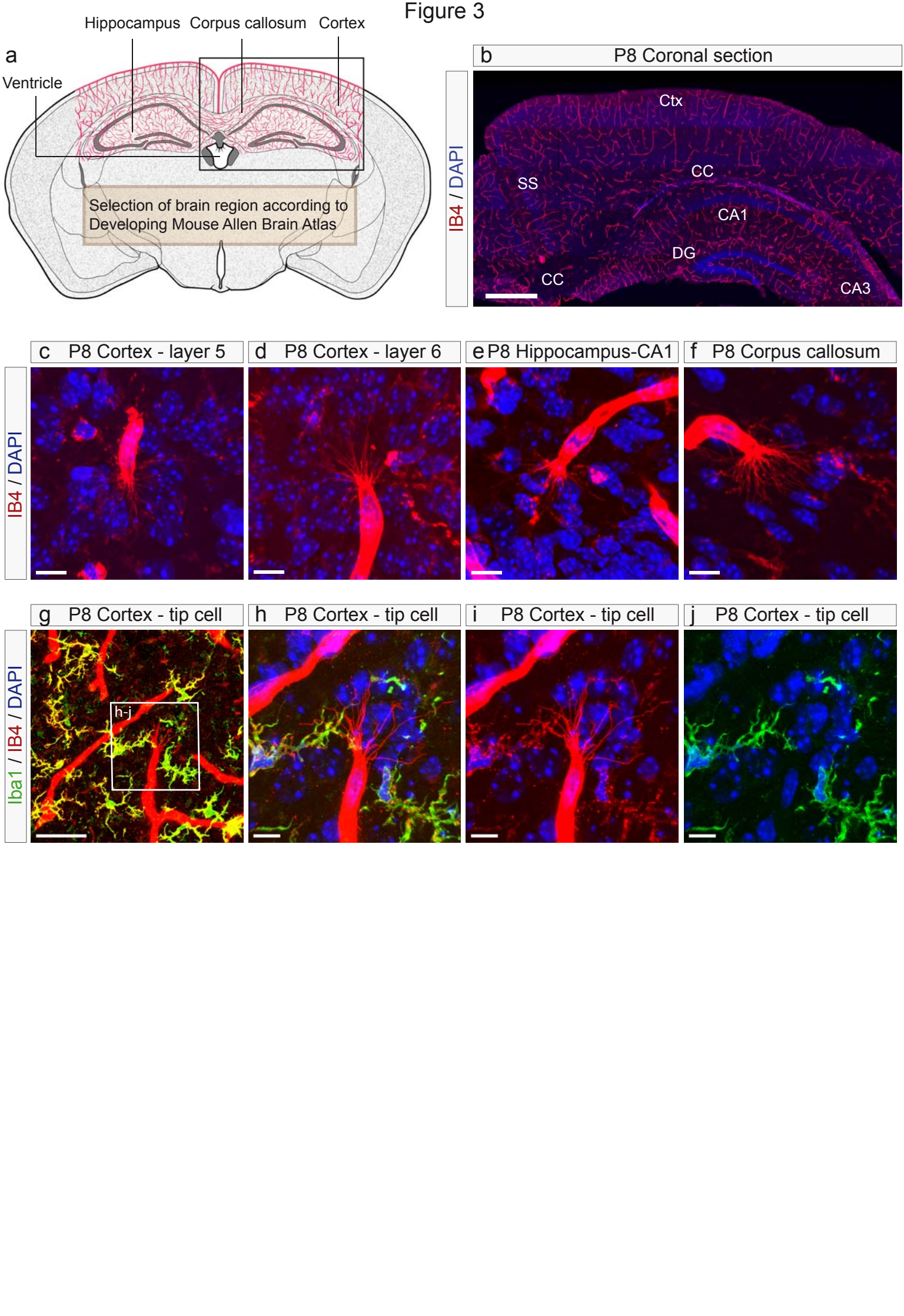
a
Hippocampus
Corpus callosum
Cortex
Ventricle
Selection of brain region according to
Developing Mouse Allen Brain Atlas
b P8 Coronal section
IB4 / DAPI
Ctx
SS
CC
CA1
DG
CC
CA3
c P8 Cortex - layer 5
d P8 Cortex - layer 6
e P8 Hippocampus-CA1
f P8 Corpus callosum
IB4 / DAPI
g P8 Cortex - tip cell
h P8 Cortex - tip cell
i P8 Cortex - tip cell
j P8 Cortex - tip cell
Iba1 / IB4 / DAPI
h-j

Figure 4

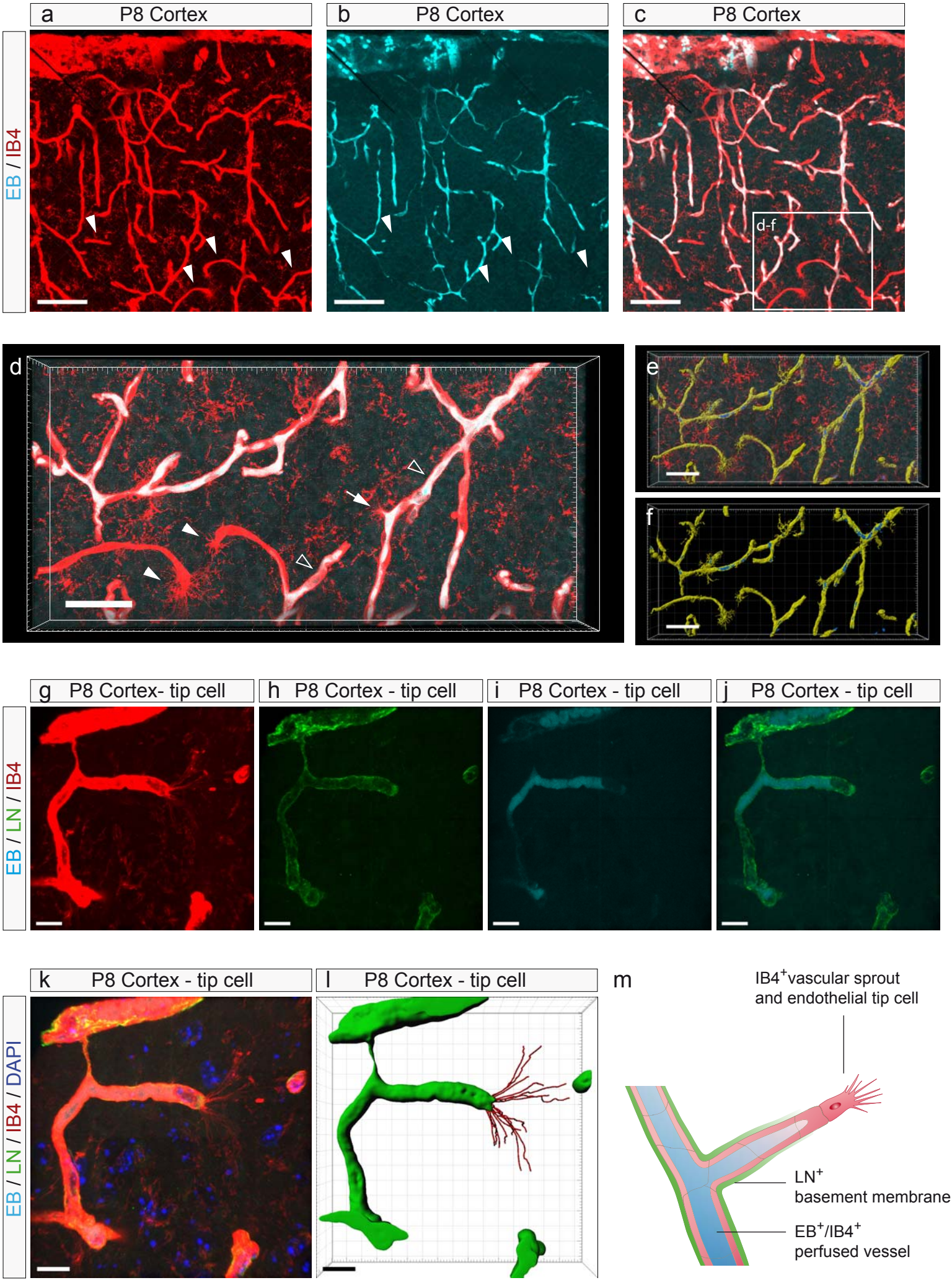
a P8 Cortex
b P8 Cortex
c P8 Cortex
EB / IB4
d-f
d
e
f
g P8 Cortex- tip cell
h P8 Cortex - tip cell
i P8 Cortex - tip cell
j P8 Cortex - tip cell
EB / LN / IB4
k P8 Cortex - tip cell
l P8 Cortex - tip cell
EB / LN / IB4 / DAPI
m
IB4+vascular sprout
and endothelial tip cell
LN+
basement membrane
EB+/IB4+
perfused vessel

Figure 5

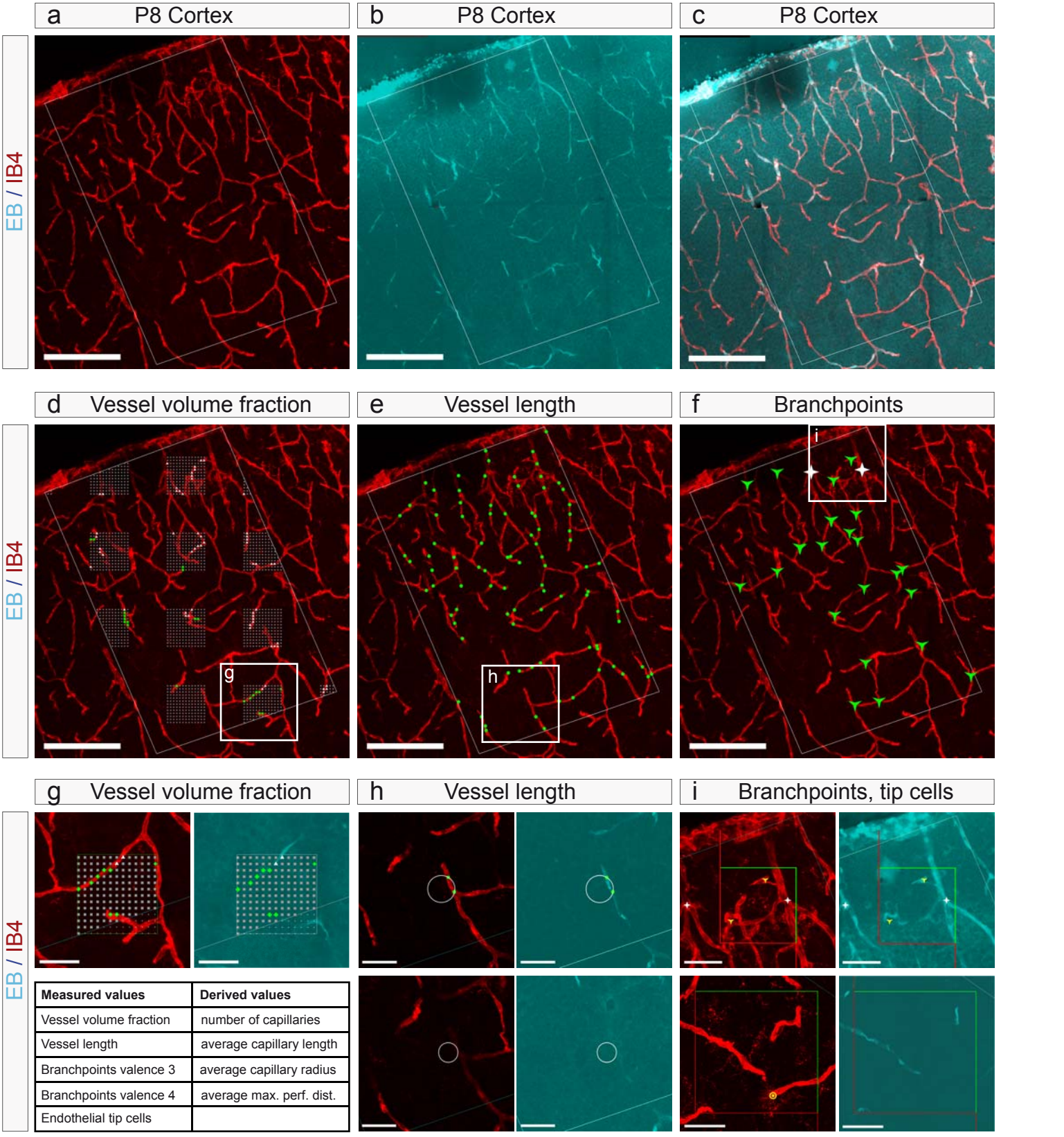

Measured values	Derived values
Vessel volume fraction	number of capillaries
Vessel length	average capillary length
Branchpoints valence 3	average capillary radius
Branchpoints valence 4	average max. perf. dist.
Endothelial tip cells	

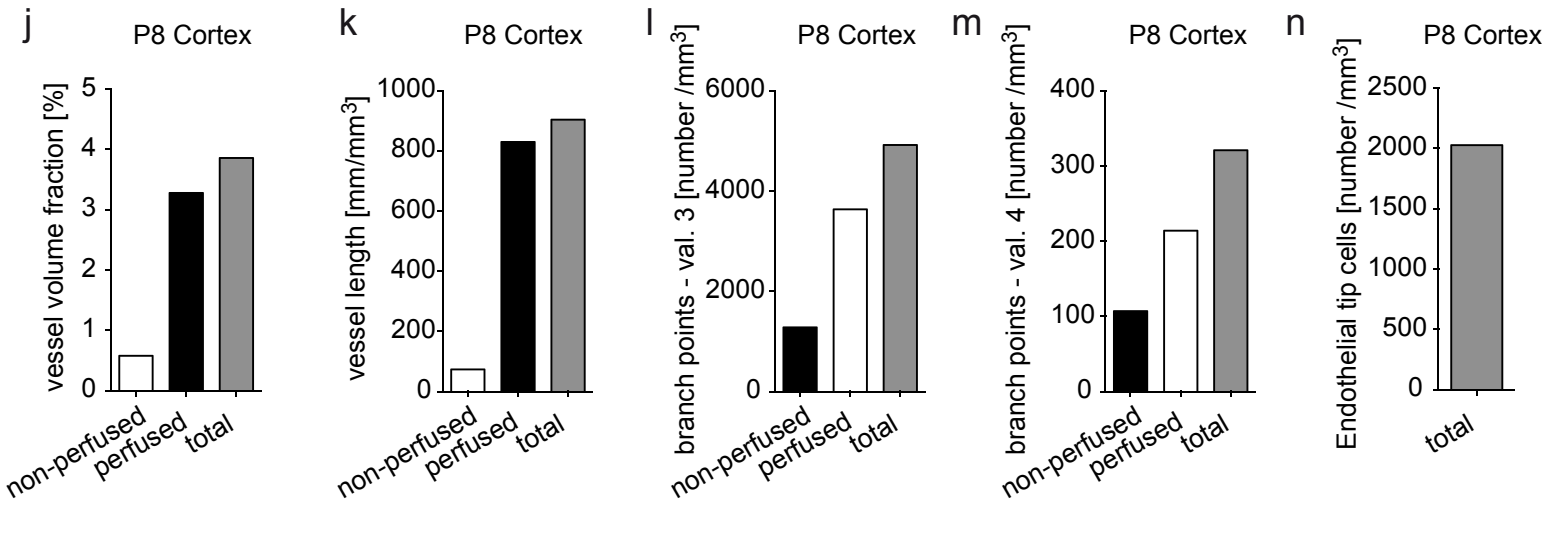

Figure 6

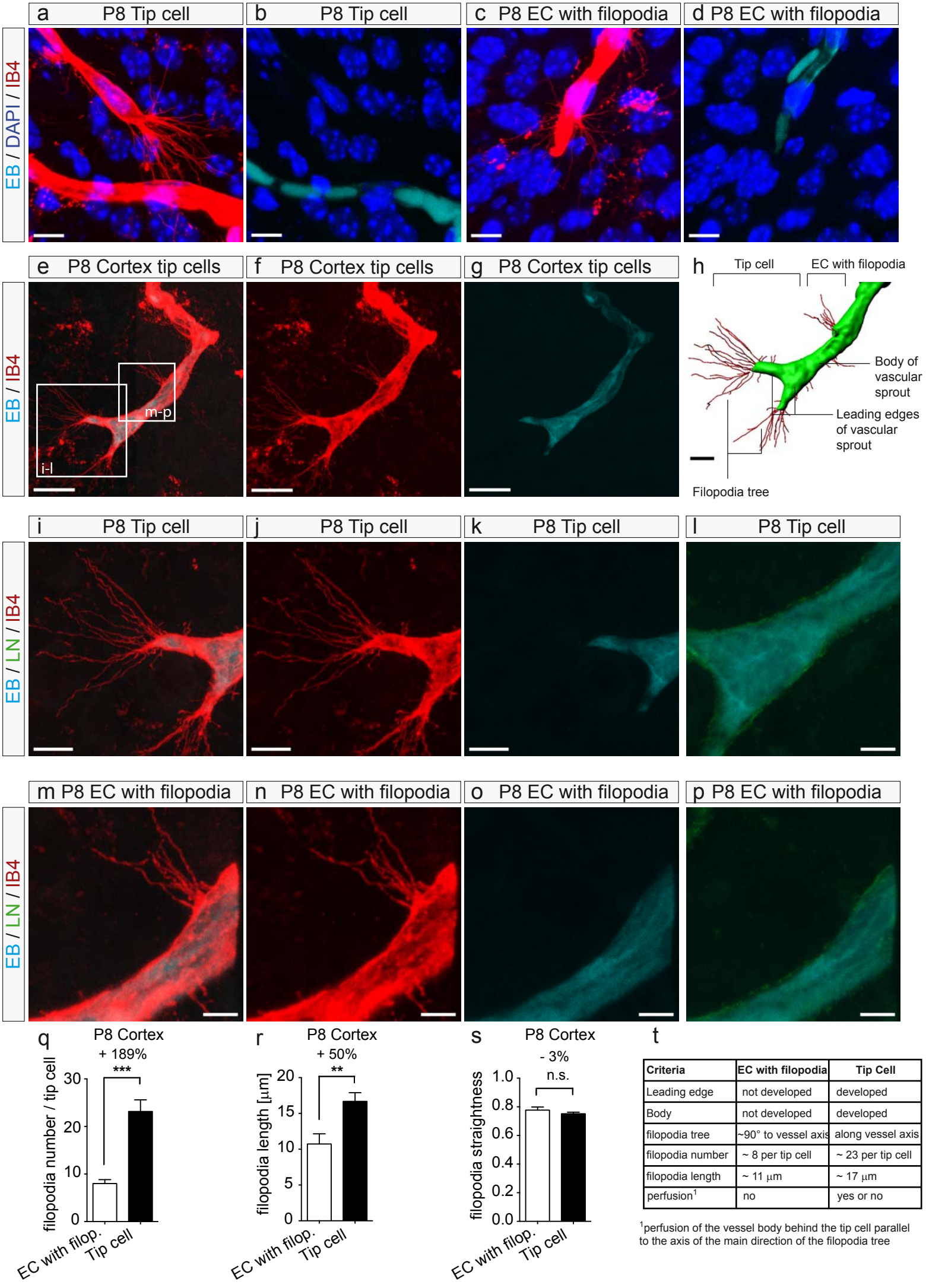

t

Criteria	EC with filopodia	Tip Cell
Leading edge	not developed	developed
Body	not developed	developed
filopodia tree	~90° to vessel axis	along vessel axis
filopodia number	~ 8 per tip cell	~ 23 per tip cell
filopodia length	~ 11 µm	~ 17 µm
perfusion[1]	no	yes or no

[1]perfusion of the vessel body behind the tip cell parallel to the axis of the main direction of the filopodia tree

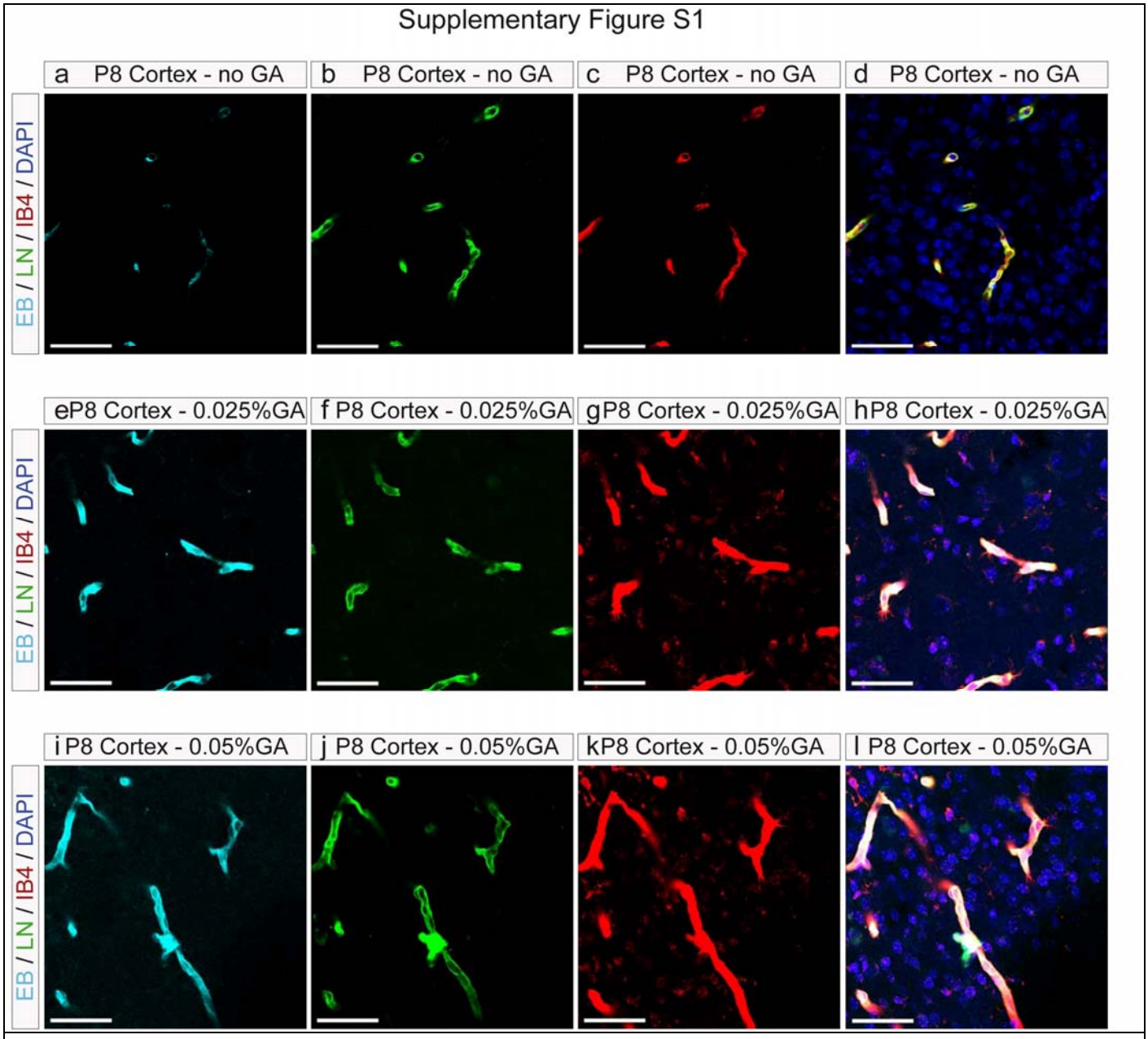

Supplementary Figure S1

Optimization of the tissue fixation protocol to combine EB-perfusion and IB4 endothelial tip cell staining in the postnatal mouse brain

a-l Labeling of EB-perfused P8 mice with biotinylated IB4 in combination with immunfluorescence (e.g. LN to label the basement membrane). Different fixation methods of EB-perfused P8 mice to optimize the combination of EB perfusion with IB4 endothelial tip cell labeling and antibody stainings were tested. Combinations of

immersion-fixation with 4% FA and different amounts of GA were used. Subsequently, 40 µm coronal brain sections were labeled with biotinylated IB4 to visualize blood vessel endothelial cells (red) and with an antibody against LN (green) to test if antigenicity is still present despite GA treatment (**a-l**,). EB (perfused blood vessels, cyan). Whereas postfixation in 4% FA only (no GA) resulted in a considerable loss of the EB signal (**a-d**), the combination of 4% FA + 0.025% GA (**e-h**) or 4% FA + 0.05% GA (**i-l**) were optimal for combination of the different label procedures (IB4, LN) with EB-perfused vessels.

Scale bars: 50 µm (**a-l**).

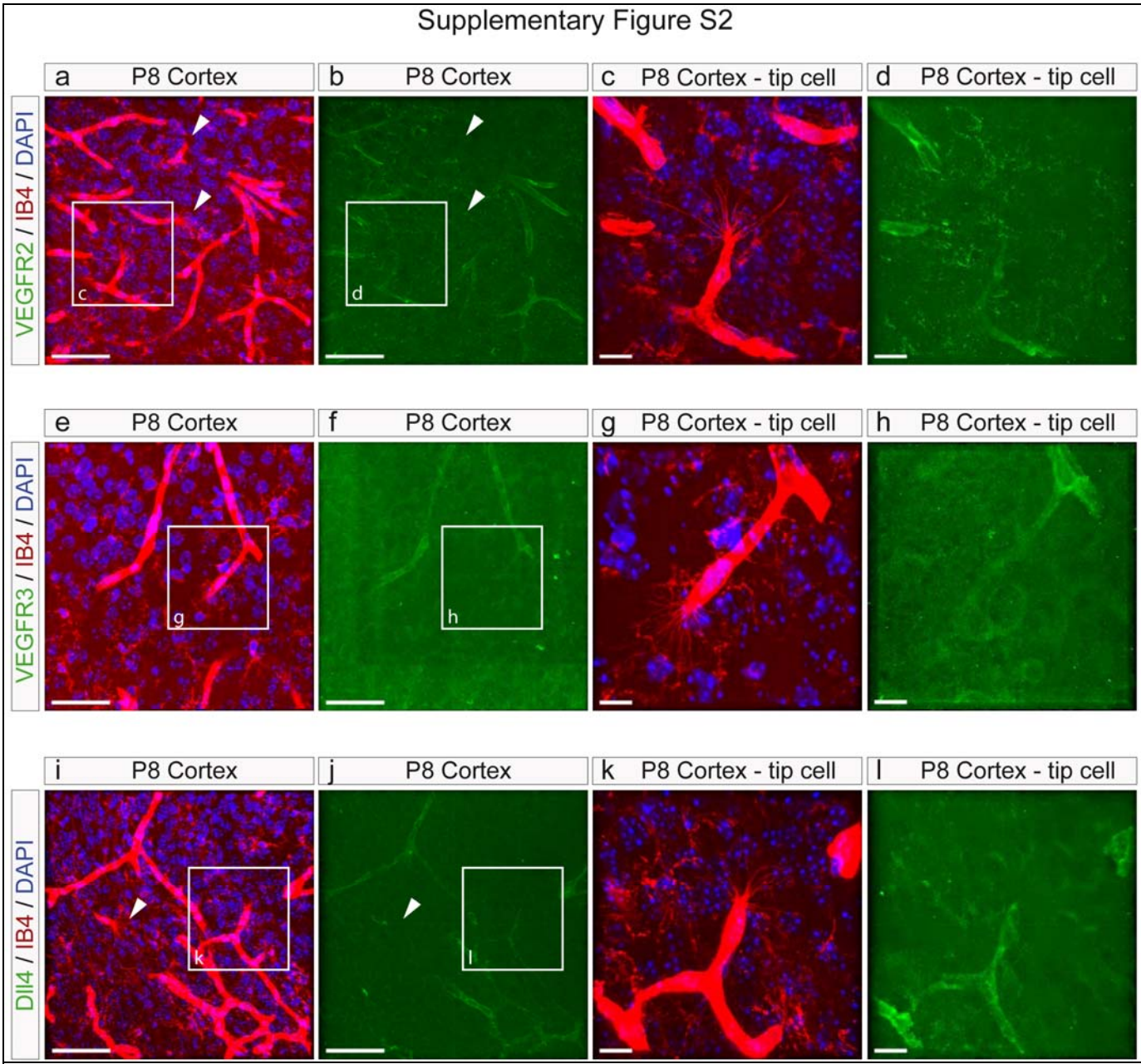

Supplementary Figure S2

Classical endothelial tip cell markers in direct comparison to IB4 labeling in the P8 mouse brain cortex

Immunofluorescent labeling of 40 µm P8 coronal mouse brain sections labeled with the classical endothelial tip cells markers VEGFR2 (**a-d**, green), VEGFR3 (**e-h**, green) and Dll4 (**i-l**, green) and with biotinylated IB4 to visualize blood vessel endothelial (tip) cells (red). Cell nuclei (DAPI, blue).

a-l IB4 as well as antibodies against VEGFR2 (**a-d**), VEGFR3 (**e-h**) or Dll4 (**i-l**) visualize CNS blood vessel structures and endothelial tip-, stalk-, and phalanx cells. Boxed areas (**a,b,e,f,i,j**) highlight endothelial tip cells that are enlarged on the right hand (**c,d,g,h,k,l**). White arrowheads (**a,b,i,j**) mark additional endothelial tip cells **c,d,g,h,k,l** $IB4^+$ endothelial tip cells with clearly identifiable, multiple filopodia forming a typical "hand-like" structure (**c,g,k**). Note that neither VEGFR2 (**d**), VEGFR3 (**h**) nor Dll4 (**l**) label endothelial tip cell filopodia as accurately as IB4. As filopodia are the key morphological criterion for identifying endothelial tip cells, the classical tip cell markers VEGFR2, VEGFR3 and Dll4 do not facilitate the identification of endothelial tip cells in the postnatal mouse brain. Moreover, none of these markers allows a clear delineation of endothelial stalk- or phalanx cells from endothelial tip cells (**d,h,l**).

Scale bars: 50 μm (**a**,**b**,**e,f**,**i,j**) ; 10 μm (**c,d**,**g,h**,**k,l**).

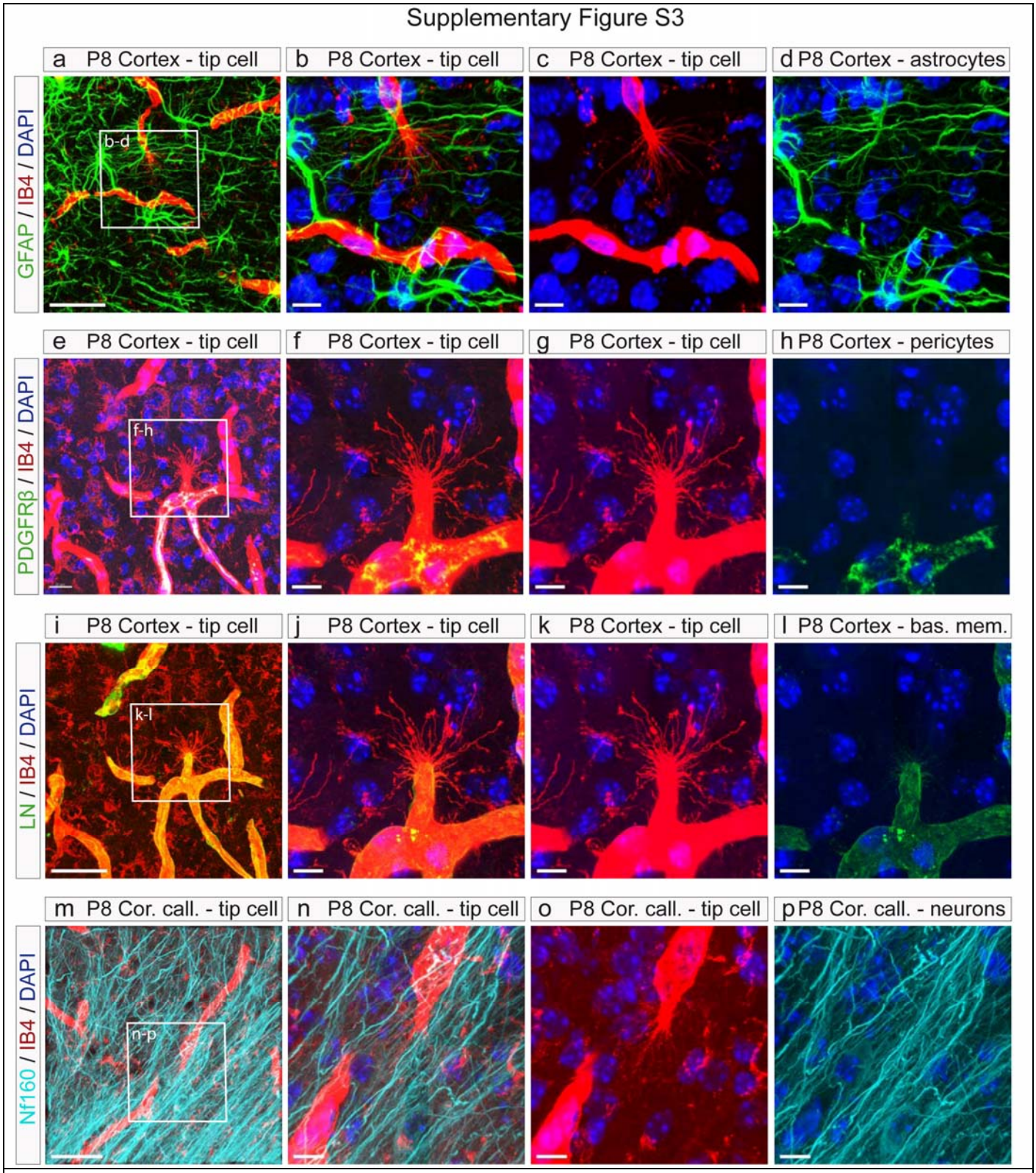

Supplementary Figure S3

Immunofluorescence of perivascular cells in vicinity of endothelial tip cells in the P8 mouse brain cortex

a-p All samples used for the immunofluorescence shown in this figure have been immersion fixed with 4% FA and 0.025% GA, which was the final fixation protocol of the present study. This ensures optimal retaining of EB inside the vessels but also good antigenicity for a variety of cellular markers (see also Supplementary Fig. S1). For example **a-d** shows $GFAP^+$ astrocytes and $GFAP^+$ radial glia (green), $IB4^+$ blood vessel endothelial cells (red) including an endothelial tip cell and an established blood vessel in the P8 mouse brain cortex. Endothelial tip cell filopodia do not follow a template of $GFAP^+$ astrocytes and radial glia (**a**). Boxed area with zoom on endothelial tip cell is enlarged in **b-d**. Cell nuclei (DAPI, blue). **e-h** $PDGFRB^+$ pericytes (green) and IB4+ blood vessels (red) in the P8 mouse cortex. Boxed area is enlarged in **f-h**. Endothelial tip cell filopodia are $PDGFRB^-$. Cell nuclei (DAPI, blue). **i-l** LN^+ (green) common basement membrane of $IB4^+$ blood vessels (red) and $PDGFRB^+$ pericytes. Boxed area with zoom on endothelial tip cell is enlarged in **j-l**. Note the faint LN-staining of endothelial tip cell filopodia at the base of the endothelial tip cell body (**l**). Cell nuclei (DAPI, blue). Note that no pericytes are present at the tip cell (f,h) whereas LN is ensheathing the tip cell body (j,l). **m-p** $Nf160^+$ axons (cyan) and IB4+ endothelial tip cell (red, filopodia) in the P8 mouse corpus callosum. Boxed area with zoom on endothelial tip cell is enlarged in **n-p**. Cell nuclei (DAPI, blue).

Scale bars: 50 μm (**a,e,i,m**); 10 μm (**b-d, f-h, j-l, n-p**).